Transportation Research Interdisciplinary Perspectives 27 (2024) 101232

Contents lists available at ScienceDirect

Transportation Research Interdisciplinary Perspectives

journal homepage: www.sciencedirect.com/journal/transportation-research-interdisciplinary-perspectives

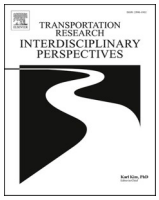

Total capacity and LOS estimation of innovative and conventional roundabouts through macroscopic fundamental diagrams

Marco Guerrieri

DICAM, University of Trento, Via Mesiano 77, 38123 Trento, Italy

A R T I C L E I N F O

Keywords:
Deterministic Macroscopic Fundamental Diagram
Conventional and Unconventional Roundabouts
Total Capacity
LOS
Traffic Simulations

A B S T R A C T

Traffic congestion remains a significant problem, especially in urban areas. To avoid congestion phenomena, several measures can be adopted, including the construction of roundabouts and the control of the measures of effectiveness (MOEs) at intersections. This article compares different types of roundabouts by estimating the deterministic fundamental diagram (MFD) and using microscopic traffic simulations. The deduction of MFD for different roundabout types (single and double-lane, flower and turbo-roundabout) is based on reasonably simplified traffic and boundary conditions. MFDs are estimated through several OD traffic matrices, considering as outputs the values of the macroscopic traffic variable deduced in time intervals of 5 min and 1 h. The findings from this research, in terms of total capacity, travel times, and level of service (LOS) estimation, may be useful for traffic and highway engineers in many realistic applications to partially face congestion phenomena in urban areas. MFDs allow us to determine the best roundabout type based on the traffic demand and represent a parsimonious method for monitoring and controlling traditional and unconventional or smart roundabouts, even in the presence of connected and automated vehicles (CAVs).

Introduction

The growing increase in traffic demand, caused by urbanization and population expansion has led to increases in traffic volumes and congestion phenomena in urban road networks (Saffari et al., 2023). Therefore, implementing adequate control strategies is a primary method to reduce saturation phenomena in urban areas, thus increasing vehicle speed and reducing vehicle density, delays, and emissions.

New research on fundamental macroscopic diagrams (MFDs) and related technical applications represents a promising method for real-time monitoring of the quality of traffic at network levels or individual road intersections. The MFD is a unimodal, low-dispersion relationship between two of the three macroscopic traffic variables: space mean speed v, vehicle density k and flow q (Geroliminis and Daganzo, 2007; Geroliminis and Daganzo, 2008; Knoop et al., 2012).

To increase the safety and capacity of road junctions and solve urban congestion phenomena in specific road network areas, traffic engineers often adopt conventional roundabouts (i.e. single-lane, double-lane roundabouts) or innovative roundabouts (e.g. turbo roundabouts and flower roundabouts). Currently, some types of roundabouts (i.e. single-lane, double-lane roundabouts) are used in several countries, while others (e.g. turbo roundabouts) have only been used in specific countries.

Roundabouts' capacity is the basic parameter for estimating other correlated traffic variables, including delays, queues and levels of service. Traditionally, different definitions and techniques to estimate the roundabout capacity are used (Mauro, 2010):

- Entry capacity (EC), is the lowest entering flow value from an entry that produces the constant existence of vehicles queuing up to enter the circulating carriageway;
- Simple Capacity (SC), is the initial value of capacity that is reached at one entry for a regular increase of the traffic demand and for a prefixed proportion of the traffic streams at the road intersection;
- Total Capacity (TC), is the sum of the flows entering from entries that are simultaneously identical to the capacity of the corresponding entries for a given proportion of the traffic streams at the road intersection.

EC, SC, and TC are almost always estimated through gap acceptance models, according to which the capacity c_i of an entry (i) is a function of the type: $c_i = f(q_i, T_c, T_f)$, where q_i is the circulating flow, T_c the critical gap and T_f the follow-up time. T_c and T_f are the psychotechnical

E-mail address: marco.guerrieri@unitn.it.

https://doi.org/10.1016/j.trip.2024.101232
Received 13 July 2024; Received in revised form 10 September 2024; Accepted 17 September 2024

parameters of users. The value of T_c cannot be directly measured by traffic records but can only be estimated by a single mean value with specific techniques, such as the Drew, Raff, Ashworth and Miller methods. (Mauro, 2010). However, these techniques simplify the real behaviour of drivers at roundabouts for the following main reasons:

- the value of T_c is heterogeneous in the population of drivers, while the acceptance gap models consider only one value, the same for all users;
- T_c is a random variable with unidentified probability law;
- drivers can modify and change T_c over time based on different traffic circumstances.

After having estimated the roundabout capacity, the control delay and the service level of service (LOS) can be calculated. The control delay is calculated with queuing theory methods. However, since in undersaturated traffic conditions ($x = q_i/c_i < 1$) stochastic models do not allow the analysis of several non-stationary events that occur in the real world (e.g. when $x \geq 0.7$–0.8) and in conditions of saturated or oversaturated traffic ($x \geq 1$) the deterministic model is not entirely applicable, in technical investigations heuristic solutions are generally used. For instance, the well-known HCM method (HCM, 2022) for control delay estimation provides formulas that are based on the heuristic solutions of Akçelik and Troutbeck provided that the arrival process and the service time follow a Poisson's law and an exponential probability distribution, respectively (Guerrieri and Mauro, 2021).

It should also be considered that closed-form capacity models, including the HCM model, assume that congestion phenomena cannot occur on the circulating lane, while in reality queues are sometimes encountered even on the ring lanes. All these hypotheses regarding traffic conditions and user behaviour only seldom happen simultaneously in real operating conditions. Therefore, the estimate of MOEs (i.e. capacity, queue, waiting time, and control delay) established on the gap-acceptance assumption can frequently be affected by inaccuracies.

Regarding macroscopic performance, the Macroscopic Fundamental Diagram (MFD) intuitively reflects how different roundabout types operate at different traffic demand levels. The MFD relates the macroscopic traffic variables (flow, space mean speed and density) based on highly aggregated data. It extends to networks or road intersections the model of the fundamental diagram (speed-flow curve) that was found by Greenshield in his pioneering scientific work (Greenshields, 1935), which is arguably the most significant quantitative characterization of traffic law in cross sections of a road.

Research on different types of roundabouts has proven their effectiveness in improving traffic operations, safety and environmental sustainability in urban areas (Fernandes and Coelho, 2023).

In light of these considerations, in this research, we attempted a new method based on MFDs for MOE measurement of different roundabout types: single-lane, double-lane, flower, and turbo-roundabout (Gellelli et al., 2016). MFDs are estimated with microscopic traffic simulations in the Aimsun environment.

This research demonstrates that the MFD can provide an alternative tool for estimating the MOEs at roundabouts (NCHRP Report, 2010; Guerrieri, 2024b; Brilon et al., 2023) able to circumvent the demand uncertainty problem of usual traffic theory models.

In particular, the contributions of this research are four-folded:

- traffic simulations are performed considering factors such as roundabout types and different demand traffic levels;
- conventional and unconventional roundabouts are studied;
- MFDs are derived by analysing unsaturated, saturated, and oversaturated traffic conditions, considering factors such as the roundabout types and traffic scenarios;
- based on the MFD, for each roundabout layout, the MOEs are estimated (i.e. Total Capacity, Travel Time, etc.) and roundabout types are compared.

The rest of the paper is arranged as follows. In Section 2 the notion of the deterministic macroscopic fundamental diagram is explained. Section 3 presents the dataset, the simulation and the calibration processes of the microscopic traffic model in the Aimsun environment. Section 4 describes discussions and results regarding MFDs for all the roundabout types analysed along with the estimated total capacities and service levels. Section 5 presents the conclusions of this research.

The deterministic macroscopic fundamental diagram for a roundabout

The most used model to describe vehicles flowing along a road infrastructure under the hypothesis of steady-state conditions is the deterministic fundamental equation whose graphical representation is the so-called Fundamental Diagram (FD) linking the relationship between three macroscopic traffic variables, namely the traffic flow q, the space mean speed v and the vehicle density: $q = k \bullet v$. FD is an equilibrium traffic flow model because it represents a steady-state or equilibrium relationship between the macroscopic traffic variables q, k and v. In particular, density-speed relationships $v = f(k)$ can be grouped into single-regime (linear or nonlinear functions, e.g. Greenshields, Greenberg, Underwood, Newell, Drake, Papageorgiou, Kerner and Konhäuser, Del Castillo and Benitez, Wang and Cheng models) and multi-regime models (e.g. Edie, Two-regime, Modified Greenberg and Three-regime models) (Lei et al). Single-regime models are not able to fit all the density ranges well; instead, multi-regime models can describe density-speed relationships throughout the entire range of density values.

The stochastic fundamental diagram model is founded on the principle that the density-speed relationship depends on the density and its distribution: $v = f(k,\omega(k))$ where k is the density and $\omega(k)$ indicates the density distribution of k. However, both stochastic and deterministic FD models are essentially regression models. The deterministic fundamental equation and its diagram can be proved for steady-state traffic situations using a generic time (t) – space(x) domain D_t as shown in Fig. 1.

By analysing Fig. 1 and denoting with ΔX, the length of a road section, Δx the segment length, n the vehicles of the traffic stream entering the segment Δx long and exit from it in the time interval ΔT, q(x) the traffic flow in section x, $\overline{v}_s(x)$ the space mean speed in the cross-section x (harmonic mean of the instantaneous vehicle speeds $v_i(x)$), k(x) the mean vehicle density, $\Theta$the occupation, the following relationships can be obtained (Lei et al):

$$q(x) = n(x)/\Delta T \tag{1}$$

$$\overline{v}_s(x) = \frac{n \cdot \Delta x}{\sum_{i=1}^{n} \Delta t_i} \tag{2}$$

$$\Theta = \frac{\sum_{i=1}^{n(x)} \Delta t_i}{\Delta T} \tag{3}$$

$$k(x) = \frac{\Theta}{\Delta x} = \frac{\sum_{i=1}^{n(x)} \Delta t_i}{\Delta T \cdot \Delta x} \tag{4}$$

$$\frac{q(x)}{\overline{v}_s(x)} = \frac{n(x)}{\Delta T} \cdot \frac{\sum_{i=1}^{n(x)} \Delta t_i}{n(x) \cdot \Delta x} = \frac{\sum_{i=1}^{n(x)} \Delta t_i}{\Delta T \cdot \Delta x} \tag{5}$$

$$q(x) = k(x) \cdot \overline{v}_s(x) \tag{6}$$

For simplicity of notation, denoting with q the flow, k the density and v the space mean speed, we obtain:

$$q = k \cdot v \tag{7}$$

Eq. (7) represents the so-called fundamental flow relationship whose graphical representation in the form $v = f(q)$ or $q = f(k)$ is the fundamental diagram (FD).

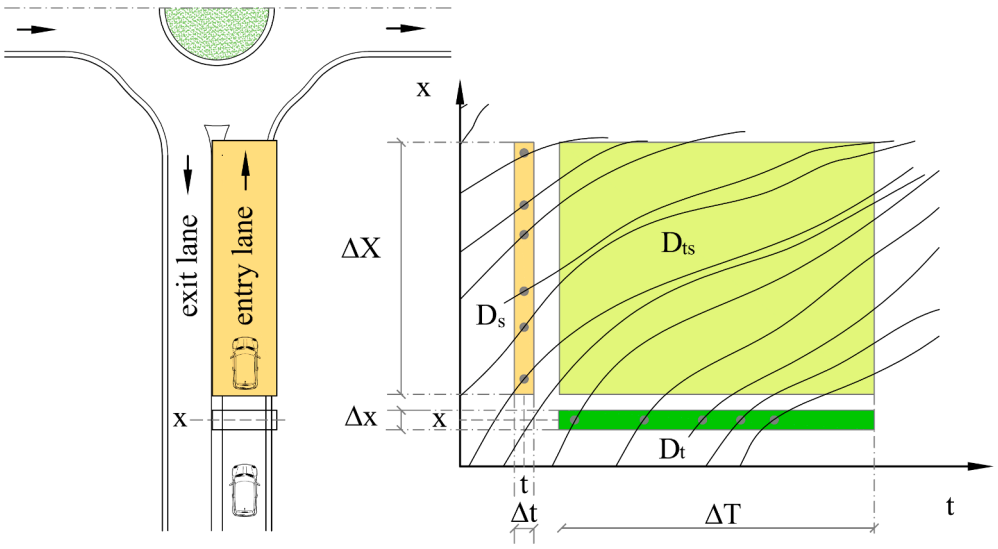

Fig.1. Time-space domain for an entry lane.

The Greenshields model is one of the best-known and most-used FDs in traffic engineering. It gives rise to a shape-bell v = v(q) curve that shows a capacity $c = q_{max}$ (i.e. the peak flow) at a certain vehicle density $k = k_c$ (i.e. critical density), q = 0 veh/h for k = 0 veh/km and a jam density $k = k_{jam}$.

In technical applications, FD is used for several purposes, including traffic regulations on highways to reduce congestion (i.e. to avoid $k > k_c$), jam and queue phenomena (i.e. to prevent the condition $k \approx k_{jam}$) or during the planning and design phases of new roads that will operate under interrupted traffic conditions.

Based on the previous demonstration (cf. Eqs.1–7), the FD should only be applied under uninterrupted and stationary traffic states. However, for practical purposes, the FD is also used by engineers in a wide range of traffic circumstances.

If the macroscopic traffic flow variables (q, v and k) are not estimated in a road section under steady-state conditions but are evaluated as mean values at the road network level, the equation that links flow, speed and density is called Macroscopic Fundamental Diagram (MFD).

Recent research provides insights into the theoretical and practical applications of MFDs in real urban networks. The theoretical and holistic method to derive a global macroscopic equation for a network with different types and numbers of roads, signal settings, and traffic demand was originally proposed by Godfrey in his pioneering study (Godfrey, 1969).

Geroliminis and Daganzo analysed real traffic data and proved the reproducible structure of MFDs for urban road networks (Geroliminis and Daganzo, 2007; Geroliminis and Daganzo, 2008). New empirical studies confirmed insights and applications of the MFD in small and big size cities (Ni et al., 2018; Zheng et al., 2016). Some research examined the existence of MFDs in road networks through traffic simulation software (Stamos et al., 2015). However, at a road network level, traffic is dynamic (i.e., not in steady-state conditions), and heterogeneity is observed in the spatial distribution of vehicles in different regions of the road network. Finally, public transport operations, priority systems, pedestrians and cyclists can interfere with vehicle traffic streams over time and space.

Therefore, the MFD must be considered an empirical formulation that is not demonstrable theoretically, whose equation is:

$$Q = K \cdot V \tag{8}$$

If a speed-density relation is assumed, it follows:

$$Q(K) = K \cdot V(K) \tag{9}$$

In which Q represents the total number of vehicles entering the cordon of the analysed road network in the observed interval of time (veh/h), K is the vehicle density averaged over the area of the cordon (veh/km) and V is the mean space speed evaluated in all the roads within the cordon (km/h).

Recently, researchers analysed the performance of conventional roundabouts with the support of MFDs, therefore, in a very different way with respect to conventional methods, which require the estimation of delays and levels of service at entries.

This study examines the derivation of MFDs for different roundabout types through microscopic traffic simulations in the Aimsun environment to estimate total capacities and other MOEs. The following layouts are examined (Fig. 2) (Coropulis et al., 2024):

- Single-lane roundabout;
- Double-lane roundabout;
- Flower roundabout with Yield-controlled right-turn lanes;
- Flower roundabout with stop-controlled right-turn lanes;
- Basic turbo roundabout.

Numerous simulations were conducted in Aimsun Next to obtain the characteristics and shapes of roundabouts' MFDs. The traffic model was calibrated using real traffic data of a single-lane and a turbo-roundabout into operation and then was applied to all the roundabout types under consideration. Also, drivers' psychotechnical parameters were assessed from real traffic samples.

The MFD allows for the study of the traffic complexity of a roundabout with a simplifying macroscopic model capable of considering the entire roundabout's behaviour by weighing the traffic conditions in the entry, exit, and ring lanes.

Model simulation and calibration

This research analyses traffic datasets with microscopic simulations to estimate MFDs of different roundabout types. Model calibration was performed for a typical conventional roundabout (diameter D=50 m and four two-lane entries and exits) and a basic turbo roundabout (D=50 m) placed in Trento (Italy) and Maribor (Slovenia) respectively (Fig. 3). Both roundabouts are sited in urban road networks with a speed limit of 50 km/h; arms have a symmetric arrangement with angles of almost 90° between them. Traffic samples were collected using fixed cameras and a drone. The kinematic parameters of vehicles and users' psycho-technical parameters were estimated through image processing techniques and deep learning algorithms. For the basic turbo roundabout the critical time was found to range from 4.03 s to 5.48 s, while the follow-up time

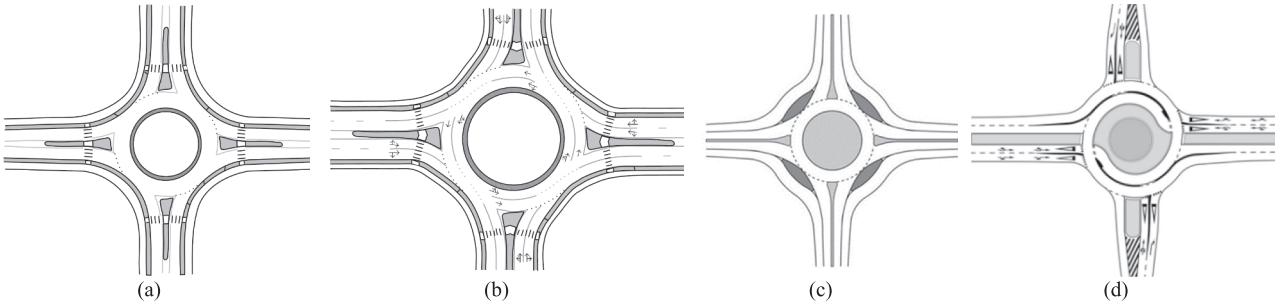

Fig.2. a) Single-lane roundabout; b) Double-lane roundabout; c) Flower-roundabout; d) Basic turbo-roundabout.

Fig.3. Roundabouts considered for the model calibration a) conventional roundabout in Trento (Italy); b) basic turbo roundabout in Maribor (Slovenia).

ranged from 2.52 s to 2.71 s.

Traffic microsimulation models are based primarily on car-following theory which establishes the kinematic interactions between two vehicles following each other in a traffic stream without overtaking manoeuvres. After the presentation of the first traffic microsimulation models in the 1950 s (i.e. Reuschel and Pipes models), many other models with more or less complex mathematical structures have been formalised. Car-following models can be grouped into three main classes (Guerrieri et al., 2015; Coropulis et al., 2024):

- Psycho-physical models;
- Safety distance models;
- Models derived from the basic Gazis-Herman-Rothary model (GHR).

In this research, traffic simulations were executed through Aimsun Next, which permits the estimation of many traffic indicators, including capacities, delays and level of services of different road and highway facilities. In Aimsun software, the Gipps (Gipps, 1981; Gipps, 1986) car-following model is implemented. The Gipps model consists of two very different equations that simulate the speeds in free-flow and not free-flow regimes (V_a and V_b respectively), as follows (Barcelo, 2010):

$$V_a(n,t+T) = V(n,t) + 2.5a(n)T\left(1 - \frac{V(n,t)}{V^*(n)}\right)\sqrt{0.025 + \frac{V(n,t)}{V^*(n)}} \qquad (10)$$

where:

- V(n, t) is the speed of the vehicle n at time t;
- V*(n) is the desired speed of the vehicle (n) for the current position;
- a(n) is the maximum acceleration for the vehicle n;
- T is the reaction time.
- d(n) (<0) is the maximum deceleration desired by vehicle n;
- x(n, t) is the position of the vehicle n at time t;
- x(n − 1, t) is the position of the preceding vehicle (n − 1) at time t;
- s(n − 1) is the effective length of the vehicle (n − 1);
- d'(n − 1) is an estimation of the vehicle (n − 1) desired deceleration.

The speed of the vehicle (n) in the interval of time (t, t + T) is obtained as:

$$V(n,t+T) = \min\{V_a(n,t+T), V_b(n,t+T)\} \qquad (12)$$

Finally, the location of the vehicle n is estimated with the following relation:

$$x(n,t+T) = x(n,t) + V(n,t+T)\cdot T \qquad (13)$$

The Gipps model results from a safety condition correlated to the space gap between leader and follower vehicles and allows the calculation of vehicles' speed in subsequent simulation steps.

In addition to the car-following model (Eqs. (10)-(13)), Aimsun incorporates other models (Barcelo, 2010), e.g. the lane-changing model

$$V_b(n,t+T) = d(n)T + \sqrt{d(n)^2T^2 - d(n)\left[2\{x(n-1,t) - s(n-1) - x(n,t)\} - V(n,t)T - \frac{V(n-1,t)^2}{d'(n-1)}\right]} \qquad (11)$$

Table 1
Common counting distributions.

Distribution	Binomial	Poisson	Negative Binomial
PMFs	$\binom{r}{n}p^n(1-p)^{r-n}$	$\frac{\mu^n}{n!}e^{-\mu}$	$\binom{n+K-1}{K-1}p^K(1-p)^n$
mean μ	$r\cdot p$	μ	$\frac{K\cdot(1-p)}{p}$
variance σ^2	$r\cdot p\cdot(1-p)$	μ	$\frac{K\cdot(1-p)}{p^2}$
$\frac{\mu}{\sigma^2}$	$(1-p)^{-1}>1$	1	$p<1$
Parameter estimation	$p=(\overline{n}-s^2)/\overline{n}$ $r=\overline{n}^2/(\overline{n}-s^2)$	$\mu=\overline{n}$	$p=\overline{n}/s^2$ $K=\overline{n}\cdot p/(1-p)$
Traffic condition	Congested traffic	Light traffic	Cyclic variation in flow

(influencing the lane-changing manoeuvre) look-ahead model and the gap-acceptance model to simulate the give-way behaviour.

Concerning the counting probability distributions and the headway distributions, the most common laws used in traffic engineering are given in Table 1 and Table 2 (Mauro, 2010).

To identify the proper probability distribution for a particular traffic study, it is required to calculate the ratio between the sample mean $\overline{n}$ and the sample variance s^2 of the random variable N(x, Δt), i.e. the number of vehicles crossing the cross-section x in the interval Δt. If it results $\overline{n}\approx s^2$ or the flow q is around 400 ÷ 500 veh/h the Possin distribution can be adopted for the counting process. It was demonstrated that the headway is an exponential random variable when the counting process follows the Poisson law (Table 2). Instead, if $q \gg 400 \div 500$ veh/h, τ is a log-normal random variable (Gerlough and Huber, 1975).

To realize good results, generally, traffic simulation tasks involve almost the following five steps (Barcelo, 2010): 1) project scope; 2) package selection; 3) data assembly and input; 4) verification and calibration; 5) alternatives analysis and conclusions.

Therefore, in this research seven main key steps were addressed for traffic simulations in the Aimsun environment:

- specify the purposes of the research and the different situations to be analysed;
- roundabouts creation and O/D matrices assignment;
- counting and headway processes choice;
- kinematic and user behaviour parameter selection and assignment;
- run traffic simulations and examine whether the model operates as expected (model verification);
- model calibration and validation (so that the microscopic traffic model better matches the traffic field measurements);
- Scenario definition and traffic modeling.

Traffic microsimulations are used to evaluate the behaviour of a road network through stochastic experiments.

Certainly, one of the most important phases is the model calibration, which aims to obtain the best possible fit between the simulated values of some traffic variables and the real ones (Gerlough and Huber, 1975; Buisson et al., 2014; Gellelli et al., 2017). This is an essential and delicate phase. Calibration is achieved by iteratively adjusting the values of one or more traffic parameters, until the simulated values are very close to the real ones. In other words, for a given traffic variable(s) it is necessary to estimate the minimum of the function: e(p) = f(M(p)-d), i.e. the differences e(p) between the simulated value(s) M(p), which depend on the parameters p, and the measured value(s) (d) (Buisson et al., 2014).

The most commonly used variables to evaluate the likelihood between simulations and real data are travel times, speeds and queue lengths.

In this study, the calibration procedure was obtained by making a comparison between the queues simulated by the traffic model and those observed in the roundabouts under consideration (Fig. 3) by fixed cameras and a drone (model "DJI Mavic mini 2"). For instance, Fig. 4 and Fig. 5 give screenshots taken from aerial videos.

For safety reasons and due to the restricted flight elevation allowed in the urban zone of Trento, the traffic conditions were examined in an area (cordon area) with a diameter of 100 m beyond the central island of the roundabout (see Fig. 4). Therefore, the examined overall length of the roundabout arms is approximately 400 m (4 x 100 m).

From the sampling of traffic data, it was possible to measure the flow of entering, leaving, and circulating in the roundabout within the analyzed cordon. These flow values were deduced in 24 successive intervals, each 15 min long. Overall, 24 Origin-Destination (O/D) matrices were obtained, which made it possible to simulate the queues (xi), which were then compared with the measured ones (y_i).

The MOEs for the analyzed roundabouts were examined under both unsaturated and saturated traffic conditions, with entry flows compatible with the Poisson distribution and the exponential distribution for counting and headway processes respectively. Therefore, these distributions were adopted in simulations.

Several goodness-of-fit metrics can be applied to estimate the complete performance of a traffic simulation model; the most used are summarized in Table 3 (Hollander and Liu, 2008; Buisson et al., 2014) where:

- x_i is the simulated measurement;
- y_i is the observed measurement;
- N is the number of measurements;
- $\overline{x}$ and $\overline{y}$ are the sample averages;
- σ_x and σ_y are the sample standard deviations.

In this research, GEH (Geoffrey E. Havers) (DMRB, 1996) is used as a Measure of goodness-of-fit (Table 3). The following steps summarise the algorithm.

Table 2
Most common headway distributions.

Distribution	Negative exponential	Shifted exponential	Erlang	Log-normal
PDF $f_\tau(\tau)$	$\lambda e^{-\lambda\tau}$	0 if $\tau<c$ $\frac{1}{\frac{1}{\lambda}-c}\exp[-(\tau-c)/(1/\lambda-c)]$ if $\tau\geq c$	$\frac{\lambda e^{-\lambda\tau}(\lambda\tau)^{K-1}}{(K-1)!}$	$\frac{1}{\tau\beta\sqrt{2\pi}}\exp\left(-\frac{(ln\tau-\alpha)^2}{2\beta^2}\right)$
mean μ	$\frac{1}{\lambda}$	$\frac{1}{\lambda}+c$	$\frac{K}{\lambda}$	$\exp(\alpha+\beta^2/2)$
variance σ^2	$\frac{1}{\lambda^2}$	$\frac{1}{\lambda^2}$	$\frac{K}{\lambda^2}$	$\exp(2\alpha+\beta^2)[\exp(\beta^2)-1]$
Parameter estimation	$\frac{1}{\lambda}=\overline{\tau}$ $\frac{1}{\lambda^2}=s^2$	$c=\overline{\tau}-\sqrt{s^2}$ $\lambda^2=\frac{1}{s^2}$	$\lambda=\frac{\overline{\tau}}{s^2}$ $K=\frac{\overline{\tau}^2}{s^2}$	$\alpha=\ln\left(\overline{\tau}/\sqrt{1+c_\tau^2}\right)$ $\beta^2=\ln(1+c_\tau^2)$ where $c_\tau^2=s^2/\overline{\tau}^2$

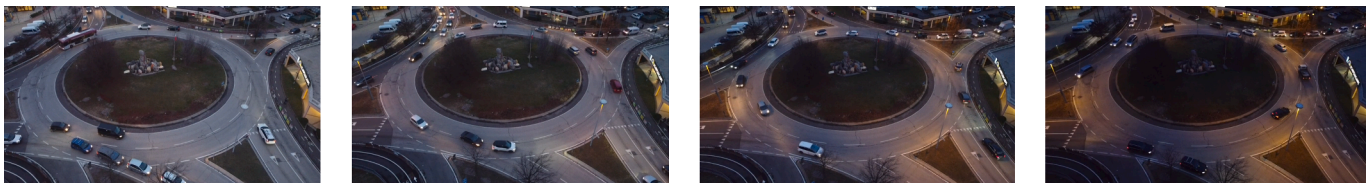

Fig.4. Screenshots of traffic video (single-lane roundabout).

Fig.5. Screenshots of traffic video (basic turbo roundabout).

$$GEH_i = \sqrt{\frac{2(x_i - y_i)^2}{x_i + y_i}} \quad (14)$$

where x_i and y_i are the *i*th simulated and observed values of queues

It then estimates an aggregated index using the following algorithm (Barcelo, 2010; DMRB, 1996):

For i = m (number of counting stations).
If $GEH_i \leq 5$, then set $GEH_i = 1$.
Otherwise set $GEH_i = 0$.
End if;
End for;
Let:

$$GEH = \frac{1}{m}\sum_{1=1}^{m} GEH_i \quad (15)$$

If GEH≥85 % then accept the model, otherwise reject the model
Endif.

In light of these considerations, specific traffic model parameters were adjusted in Amisun through an iterative process (i.e. a sensitivity analysis (Vaiana et al., 2013) to find simulation output in terms of queues close to the observed values.

Since the traffic simulation focused on road intersections, the model was calibrated by adjusting some parameters, including the acceleration and deceleration values, and setting the maximum vehicles speed to 50 km/h.

In previous studies carried out on the urban network of Trento, the use of test vehicles equipped with accelerometers and data recording systems allowed the following values to be estimated:

- maximum acceleration: 3.10–4.10 m/s^2 (default values in Aimsun: 2.60–3.40 m/s^2);
- normal deceleration: 3.70–4.90 m/s^2 (default values in Aimsun: 3.50–4.50 m/s^2).

The main outcomes of the fine-tuning parameter process are: speed acceptance = 1.00; time gap = 1.00; max acceleration = 4.10 m/s^2; safety margin factor = 1.00; sensitivity factor = 1.00.

Traffic simulations were performed with the 24 O/D matrices. The results of the simulated (x_i) and measured (y_i) queues are shown in Fig. 6 for each of the four arms. The traffic simulation model was accepted, as the GEH statistic was found to be 91%, exceeding the minimum acceptable value of 85%. A similar calibration procedure was considered for the basic turbo roundabout case study.

MFDs deduction

In this research, the Macroscopic Fundamental Diagrams (MFDs) were derived for the following roundabout types, all with a maximum inscribed diameter of 50 m (Fig. 2):

- Single-lane roundabout;
- Double-lane roundabout;
- Flower roundabout with Yield-controlled right-turn lanes;
- Flower roundabout with stop-controlled right-turn lanes;
- Basic turbo roundabout.

The detailed layouts of these roundabouts were established in Aimsun (Fig. 7) considering the configuration of the existing intersections of Fig. 3a (urban area with a speed limit of 50 km/h) that was first analysed for calibrating the microscopic traffic model with the methodological approach explained in the previous section.

MFDs were estimated for two different traffic distribution scenarios:

- *Scenario 1* ("balanced – b"): identical flow values at the four entries and a traffic distribution matrix (i.e. origin/destination percentage matrix) $PO/D^{(1)}$ in which traffic distributions were set to 33,33 % for right turns, 33,33 % for left turns and 33,33 % for through movements;
- *Scenario 2* ("unbalanced – ub"): identical flow values at the four entries and a traffic distribution matrix $PO/D^{(2)}$ in which traffic distributions were set as follows, 60 % for right turns, 20 % for left turns and 20 % for through movements.

Once an entry traffic demand (expressed by a vector) is assigned $Q_e(m) = [Q_{ei}(m)]$ – with i = 1, 2, 3, 4 – numerous Origin/Destination traffic matrices can be obtained from the following conditions:

- Scenario 1:

$$MO/D^{(1)}(m) = PO/D^{(1)} \cdot Q_e(m) = \left[Q_{ij}(m)\right], i,j = 1,2,3,4 \quad (16)$$

- Scenario 2:

$$MO/D^{(2)}(m) = PO/D^{(2)} \cdot Q_e(m) = \left[Q_{ij}(m)\right], \ i,j = 1,2,3,4 \quad (17)$$

in which $Q_{ij}(m)$ is the traffic volume that enters from the generic arm "i" and exits from the generic arm "j" of the roundabout, computed starting from the entry traffic demand $Q_e(m)$, expressed in passenger car units per hour (pc/h or pcu/h).

To obtain the most exhaustive outcomes possible, numerous traffic

Table 3
Measures of goodness-of-fit (Buisson et al., 2014; Hollander and Liu, 2008).

Method n.	Name	Measure	Notes
1	Percent error	$PE = \frac{x_i - y_i}{y_i}$	–
2	Squared error (SE)	$SE = \sum_{i=1}^{N}(x_i - y_i)^2$	–
3	Mean error (ME)	$ME = \frac{1}{N}\sum_{i=1}^{N}(x_i - y_i)$	–
4	Mean normalized error (MNE)	$MNE = \frac{1}{N}\sum_{i=1}^{N}\frac{(x_i - y_i)}{y_i}$	–
5	Mean absolute error (MAE)	$MAE = \frac{1}{N}\sum_{i=1}^{N}\lvert x_i - y_i\rvert$	–
6	Mean absolute normalized error (MANE)	$MANE = \frac{1}{N}\sum_{i=1}^{N}\frac{\lvert x_i - y_i\rvert}{y_i}$	–
7	Exponential mean absolute normalized error (EMANE)	$EMANE = A \bullet e^{-B \bullet MANE}$	A, and B are parameters.
8	Root mean squared error (RMSE)	$RMSE = \sqrt{\frac{1}{N}\sum_{i=1}^{N}(x_i - y_i)^2}$	–
9	Route mean squared normalized error (RMSNE)	$RMSNE = \sqrt{\frac{1}{N}\sum_{i=1}^{N}\left(\frac{x_i - y_i}{y_i}\right)^2}$	–
10	GEH statistic	$GEH = \sqrt{\frac{2(x_i - y_i)^2}{x_i + y_i}}$	–
11	Correlation coefficient (r)	$r = \frac{1}{N-1}\sum_{i=1}^{N}\frac{(x_i - \overline{x}) \bullet (y_i - \overline{y})}{\sigma_x \sigma_y}$	–
12	Theil's bias proportion (U_m)	$U_m = \frac{N(\overline{y} - \overline{x})^2}{\sum_{i=1}^{N}(y_i - x_i)^2}$	–
13	Theil's variance proportion (U_s)	$U_s = \frac{N(\sigma_x - \sigma_y)^2}{\sum_{i=1}^{N}(y_i - x_i)^2}$	–
14	Theil's covariance proportion (U_c)	$U_c = \frac{2(1-r) \bullet N \bullet \sigma_x \sigma_y}{\sum_{i=1}^{N}(y_i - x_i)^2}$	–
15	Theil's inequality coefficient (U)	$U = \frac{\sqrt{\frac{1}{N}\sum_{i=1}^{N}(x_i - y_i)^2}}{\sqrt{\frac{1}{N}\sum_{i=1}^{N}y_i^2} + \sqrt{\frac{1}{N}\sum_{i=1}^{N}x_i^2}}$	–
16	Kolmogorov-Smirnov test	$K-S = \max(\lvert F_x - F_y\rvert)$	F is the cumulative probability density function of x or y
17	Moses' test and Wilcoxon test	–	The procedure is described in (Kim et al., 2005)

conditions were analysed. In total, m = 45 origin–destination traffic matrices were used for simulating each scenario, assigning $Q_e(m)$ values in the range 1–1.225 pc/h, with progressive traffic increments of 25 pc/h.

The macroscopic traffic variables – flow Q, space mean speed V, and density K – were estimated considering time intervals of 15 min and 1 h. The traffic simulations allowed the creation of a big sample of traffic outputs starting from the m = 45 O/D matrices used in the study of the two scenarios described above.

The first significant result can be immediately deduced from Figs. 8 and 9. All these graphs demonstrate that the total inflow and outflow volumes are similar, especially for medium–low total flow values (e.g. around 2,000 pc/h and around 2,500 pc/h for the single-lane roundabout and the double-lane roundabout, respectively). This occurs because when the total inflows are of medium–low value, the vehicles travel through the roundabout without accumulating a significant delay. See (Fig. 10).

Instead, in the higher flow range, the deviations between the outflow and inflow volumes increase more and more as the total incoming flow approaches the capacity value of the roundabout. However, even in this field (i.e. for undersaturated or close to saturated conditions), the differences between total inflow and total outflow are not notable (percentage variations rarely reach ± 5 %).

The DMFs should be deduced by referring to the outflow volumes, given that for high vehicle density values, numerous vehicles are temporarily stored in queues which can extend beyond the cordon, and this leads to the condition that the inflow is always more than or equal to the outflow, as can be seen from Figs. 11 and 12.

However, for a better comparison with the MOEs estimation procedures (e.g. entry capacity, simple capacity and total capacity) in this article, the DMFs and capacity values were deduced considering the total Q_T inflow sample data (Guerrieri, 2024a). In fact, in traditional methods, the MOEs are deduced solely based on the total inflow volume.

However, this choice does not lead to significant distortions in determining the DMFs because the traffic microsimulations were performed in undersaturated or close to saturated conditions (i.e. under the condition: total outflows ≈ total inflows). Then, in the present study, MFDs are associated only with the total inflow Q_T.

From the numerous traffic simulations, it was possible to find an assortment of values of the following main traffic variables: inflowing volume (Q_T) and outflowing traffic volumes, vehicle density (K), harmonic mean speed (V), vehicles at inside and outside the cordon under analysis, the delay time and the total travel time. For the MFDs deduction the pairs (V; K), (Q_T; K), (V; Q_T) were collected for time intervals ΔT = 5 min and ΔT = 1h. Then, the speed-density, inflow-density and speed-inflow relationships were estimated.

Results and discussions

The true MFD of each analysed roundabout can be evaluated if the flows and densities are known. In this regard, simulations allow the generation and analysis of several traffic conditions, but for the aims of this research, only uncongested and congested traffic states are considered.

Figs. 12-21 represent the simulated pairs (V; K), (Q_T; K), (V; Q_T), which were collected for time intervals ΔT = 5 min, taking into consideration each roundabout type and scenario. Starting from the simulated macroscopic traffic variables, the MFDs were estimated and exposed in the form of the equations V = f (Q_T) (Fig. 12b-21b) and Q_T = f (K) (Fig. 12c-21c).

By analysing the MFDs, it is found that the experimental values are distributed similarly to what happens in the traditional fundamental flow diagram (FD), especially in stable flow conditions (upper portion of the diagrams). However, there are notable differences between MFDs and FDs. In fact, in the MFDs for high vehicle density values, the space mean speed (V) and the inflowing volume (Q_T) do not tend to be zero under high-density values.

This happens since V is estimated by considering the average speed of all the vehicles inside the cordon, i.e. the speed of the vehicles in the traffic streams entering, circulating and exiting the roundabouts. While the speed in the entry lanes may tend to zero for high density, the speed of vehicles in the exit lanes tends to be close to the free-flow speed (50 km/h); consequently, the space mean speed inside the cordon will never reach the value 0 km/h.

The scatter points in the graphs (V, Q_T) and (Q_T, K) display a total inflow Q_T constraint that represents the total roundabout capacity (C).

In this research, the single-regime Greenshields' density-speed relationships V = f(K) (Greenshields, 1935) was applied and drawn for interpreting the simulated traffic data because the simulated pairs' speed-density (V; K) are linearly correlated as illustrated in Fig. 12a-21a.

To assess the accuracy of the estimated linear model V = f(K) and quantify the linear model's closeness to the experimental, the R^2 (coefficient of determination) was calculated for each roundabout type and

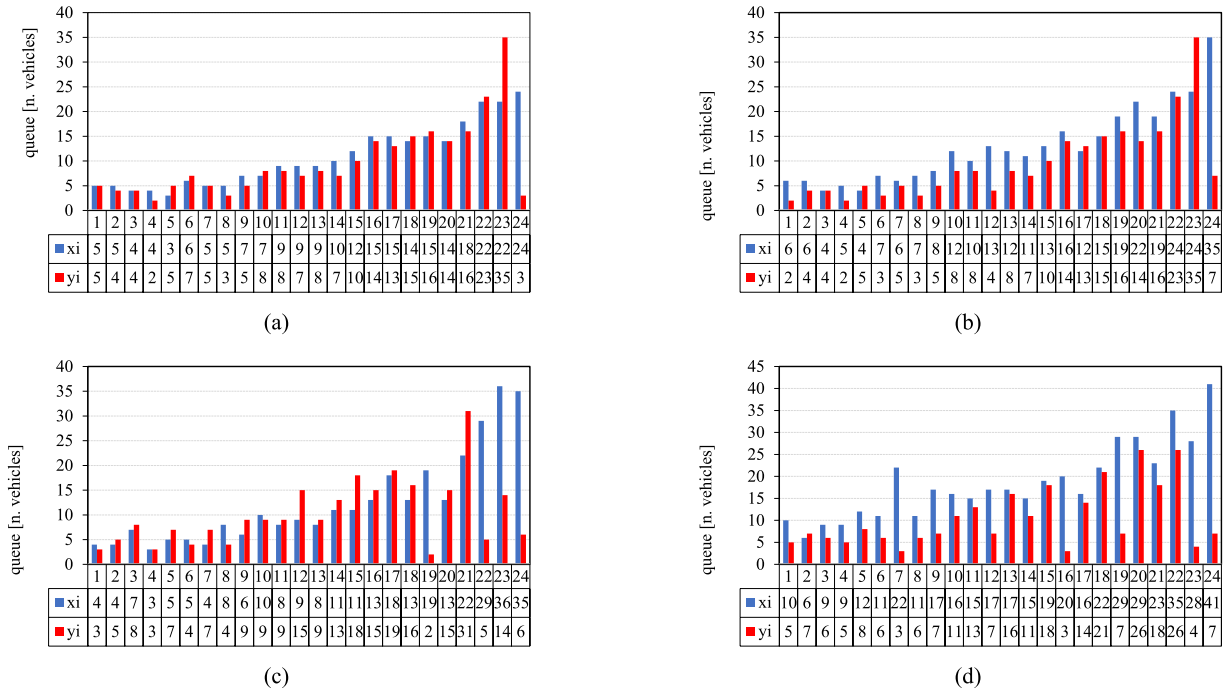

Fig.6. Measured (y_i) and estimated (x_i) queues (24O/D traffic matrices) for the conventional roundabout of Fig.4 a) Arm 1; b) Arm 2; c) Arm 3; d) Arm 4.

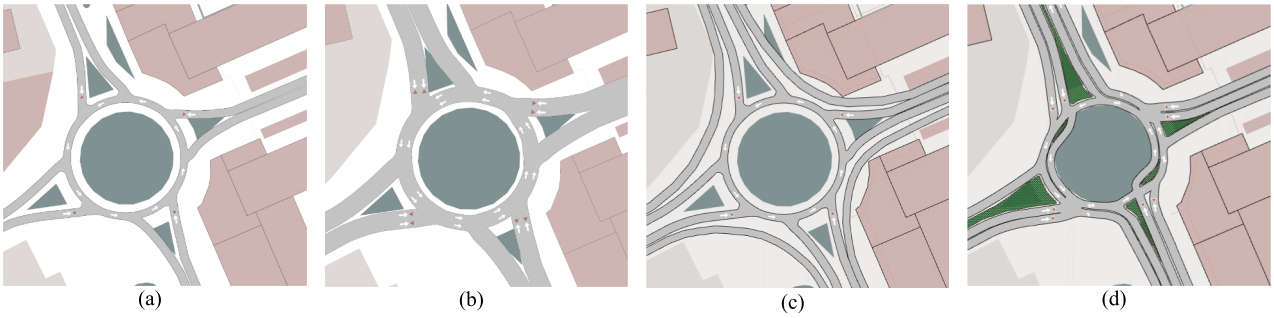

Fig.7. Analysed roundabouts in the Aimsun environment. a) Single-lane roundabout, b) Double-lane roundabout, c) Flower roundabout, d) Basic turbo roundabout.

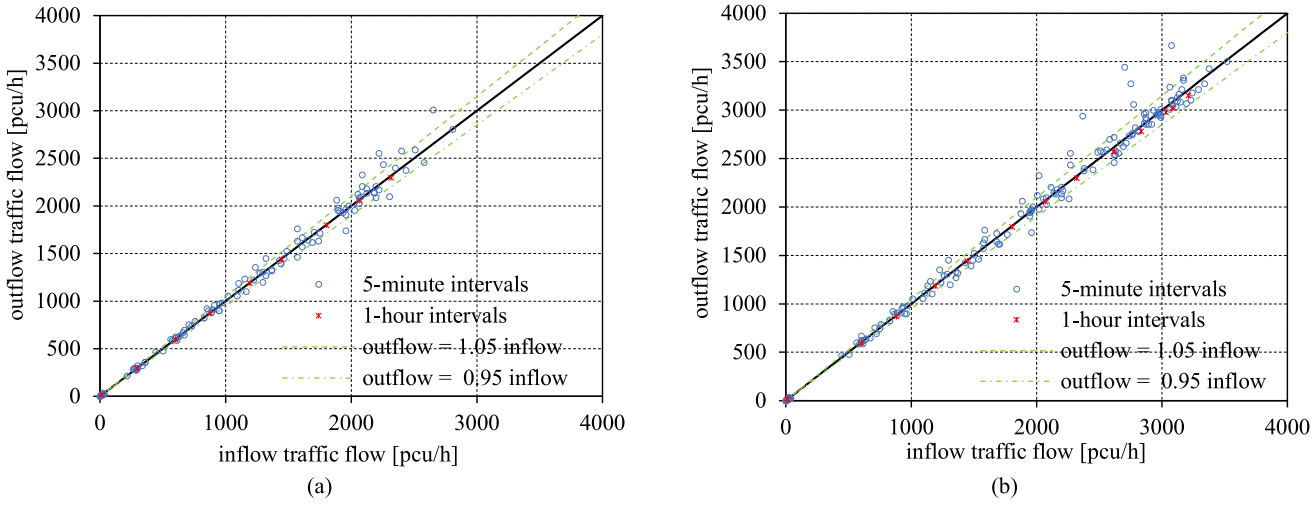

Fig.8. Inflow vs outflow values. Single and Double-lane roundabout – *Scenario 1* ("balanced – b").

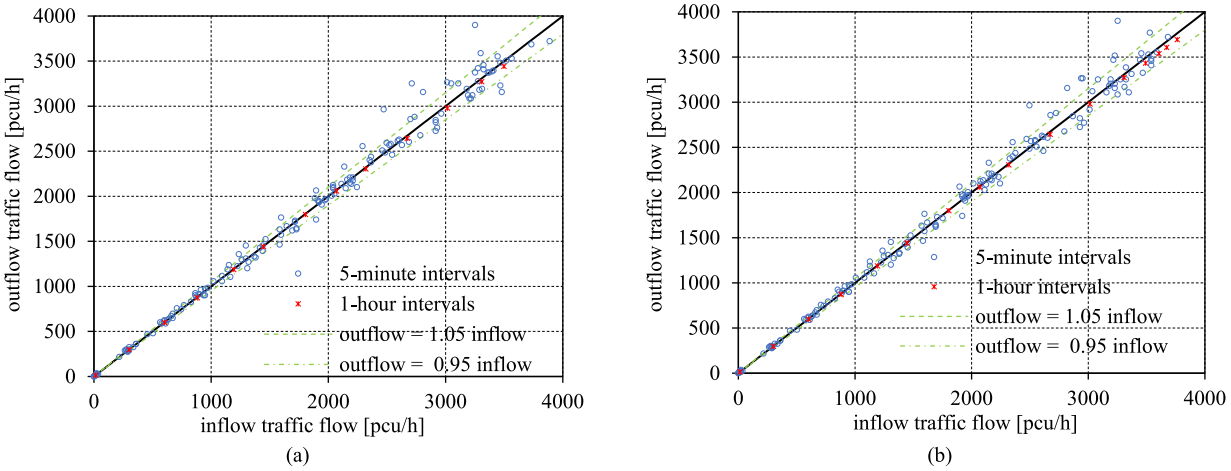

Fig.9. Inflow vs outflow values. Flower roundabout (Yield) – *Scenario 1* ("balanced – b"). Basic turbo Roundabout – *Scenario 1* ("balanced – b").

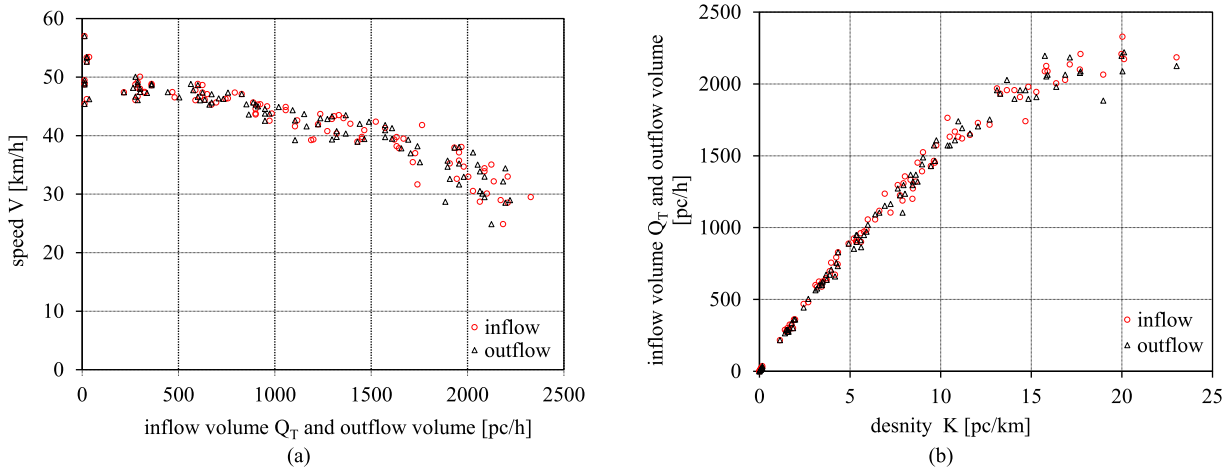

Fig.10. Speed-flow and flow-density scatter points – Single-lane roundabout, Scenario 1 ("balanced – b").

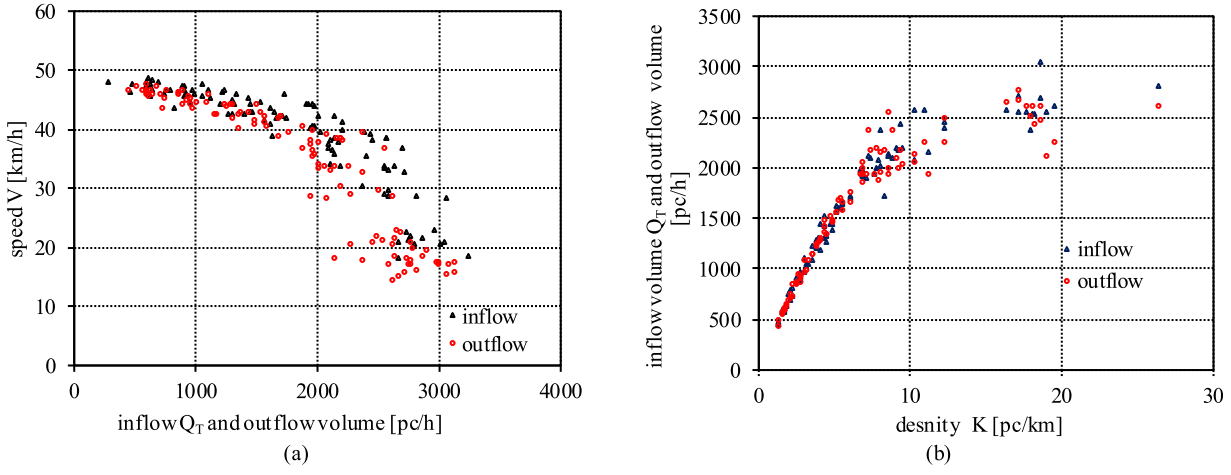

Fig.11. Speed-flow and flow-density scatter points – Double-lane roundabout, Scenario 1 ("balanced – b").

scenario. In almost all cases analysed, it turns out that $R^2>0.9$.

In the Greenshields' model, the relation V = f(K) is a bell-shaped curve by which the total capacity C and the critical density (K_c) can be immediately deduced.

The Greenshields' equation can be expressed as follows (Fig. 12a-21a):

$$V = V_f - |\beta| K \quad (18)$$

Denoting with n and l the number of arms and lanes respectively by the fundamental flow equation (Eq. (8)), the total inflow Q_T can be determined with the relationship $Q_T = Q_T(K)$, as follows:

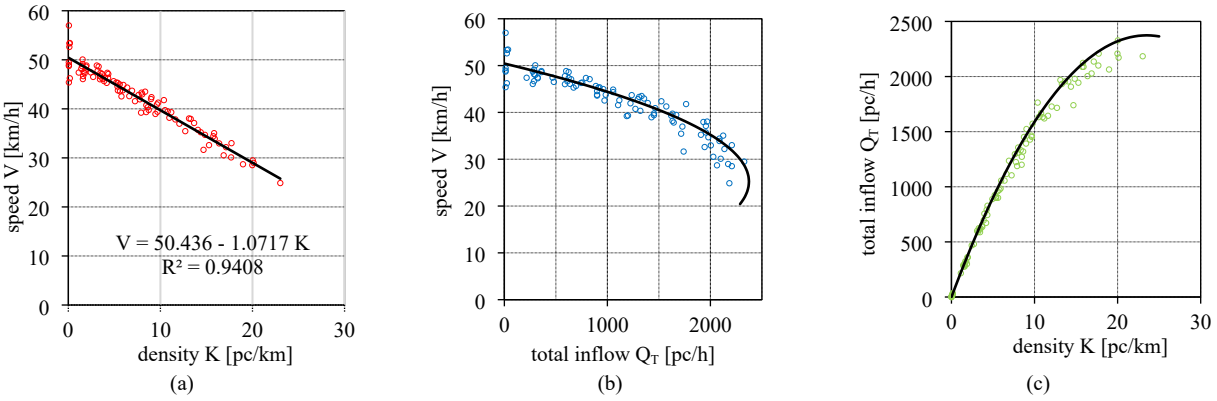

Fig.12. Scatter plots of macroscopic traffic variables and calibrated single-regime Greenshields' traffic model. Single-lane roundabout – *Scenario 1* ("balanced – b").

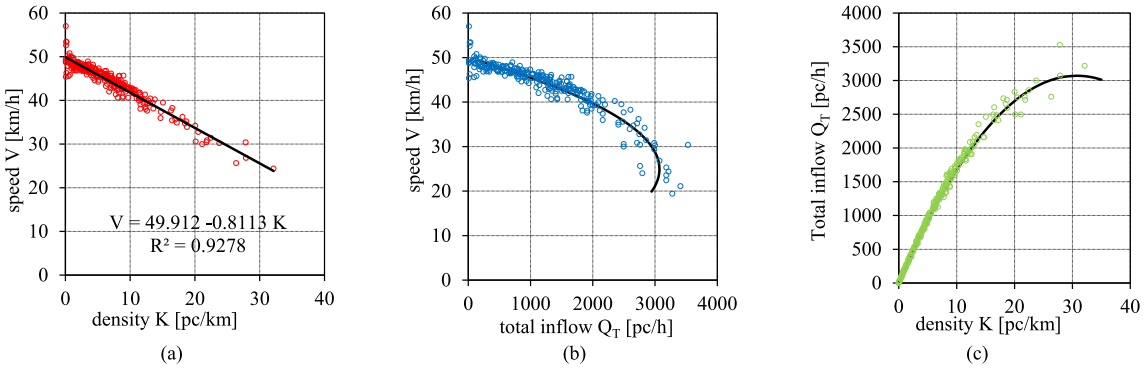

Fig.13. Scatter plots of macroscopic traffic variables and calibrated single-regime Greenshields' traffic model. Single-lane roundabout – *Scenario 2* ("unbalanced – ub").

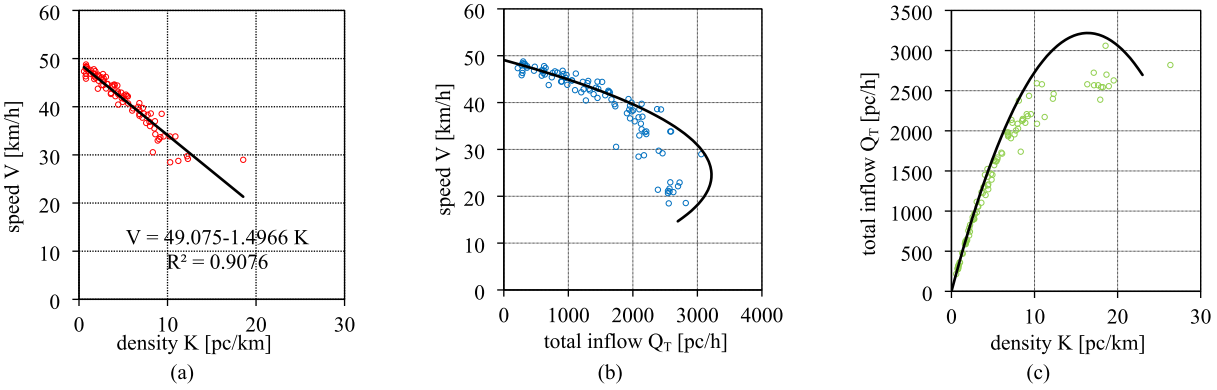

Fig.14. Scatter plots of macroscopic traffic variables and calibrated single-regime Greenshields' traffic model. Double-lane roundabout – *Scenario 1* ("balanced – b").

$$Q_T = n \cdot l \cdot V \cdot K \tag{19}$$

$$Q_T = n \cdot l \cdot (V_f - |\beta| K) \cdot K = n \cdot l \cdot V_f \cdot K - n \cdot l \cdot |\beta| \cdot K^2 \tag{20}$$

The critical density K_c is derived from Eq. (20) by imposing $Q_T^{'} = 0$

$$Q_T^{'} = n \cdot l \cdot V_f - 2 \cdot n \cdot l \cdot |\beta| \cdot K \tag{21}$$

$$Q_T^{'} = n \cdot l \cdot V_f - 2 \cdot n \cdot l \cdot |\beta| \cdot K = 0 \tag{22}$$

$$K = K_c = \frac{V_f}{2|\beta|} \tag{23}$$

Finally, the total capacity C of each roundabout is obtained by Eq. (20) and Eq. (23). Under the state to satisfy $K = K_c$, it results $C = \max(Q_T)$:

$$C = n \cdot l \cdot \left(V_f - |\beta| \cdot K_c\right) \cdot K_c \tag{24}$$

$$C = \frac{n \cdot l \cdot V_f^2}{4|\beta|} \tag{25}$$

Since the capacity C is obtained through an MFD, its physical meaning is "the maximum total inflow referred to a given period of time which has a sufficient probability of not being exceeded at a roundabout".

Eq. (25) can be used to calculate C. For instance, Eq. (25) can be specialized as follows:

- $n = 4$, $l = 1$ (4 arms single-lane roundabout):

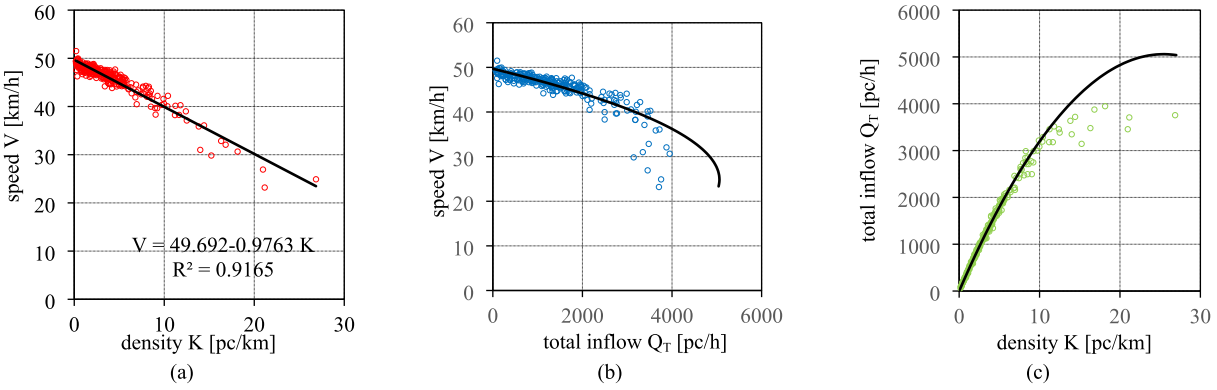

Fig.15. Scatter plots of macroscopic traffic variables and calibrated single-regime Greenshields' traffic model. Double-lane roundabout – *Scenario 2* ("unbalanced – ub").

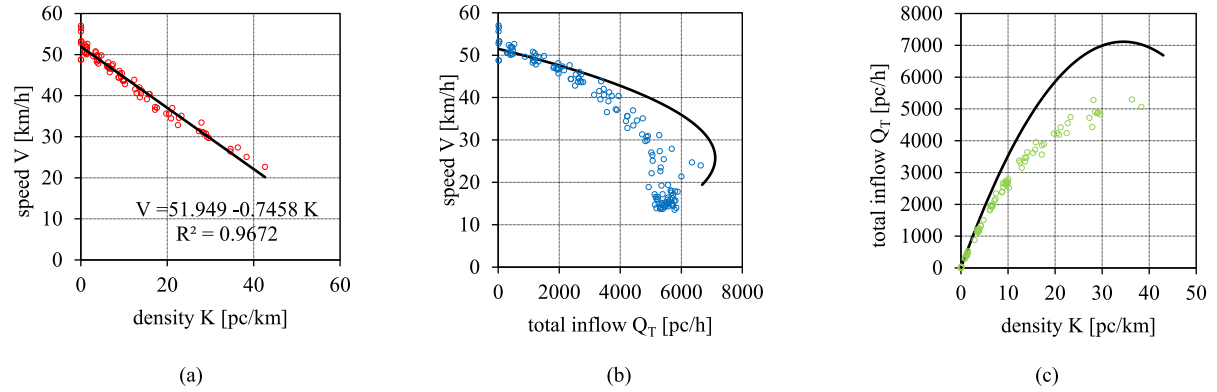

Fig.16. Scatter plots of macroscopic traffic variables and calibrated single-regime Greenshields' traffic model. Flower roundabout (Yield) – *Scenario 1* ("balanced – b").

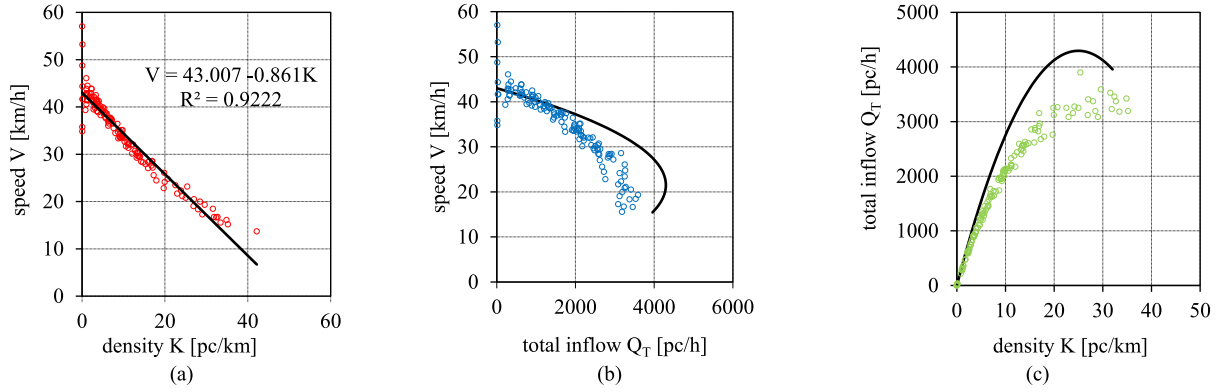

Fig.17. Scatter plots of macroscopic traffic variables and calibrated single-regime Greenshields' traffic model. Flower roundabout (Yield) – *Scenario 2* ("unbalanced – ub").

$$C = \frac{V_f^2}{|\beta|} \tag{26}$$

- $n = 4, l = 2$ (4 arms double-lane roundabout):

$$C = \frac{2 \cdot V_f^2}{|\beta|} \tag{27}$$

Tables 4 and 5 summarise the estimated V-K relations, the values of the critical density K_c, and the total capacity C for each roundabout and scenario studied. Different layouts give rise to very different capacity values , varying from a minimum of 2374 pc/h to a maximum of 7112 pc/h, depending on the roundabout type and scenario. It is evident that the single-lane roundabout gives lower total capacity and LOS and, therefore, can be adopted only in areas with low-medium traffic demand levels. Instead, double-lane and turbo roundabouts are more appropriate for medium–high traffic demand areas. In the case of Scenario 1, double-lane roundabouts, basic turbo roundabouts and flower roundabouts offer different capacity values (3233 pc/h, 4324 pc/h and 4726 pc/h, respectively). Under unbalanced traffic conditions, when right-turn manoeuvres prevail (Scenario 2), the total capacity of flower roundabouts with yield-controlled right-turn lanes is very high, reaching 7112 pc/h. This circumstance is attributable to the bypass lanes, which help reduce entry delays.

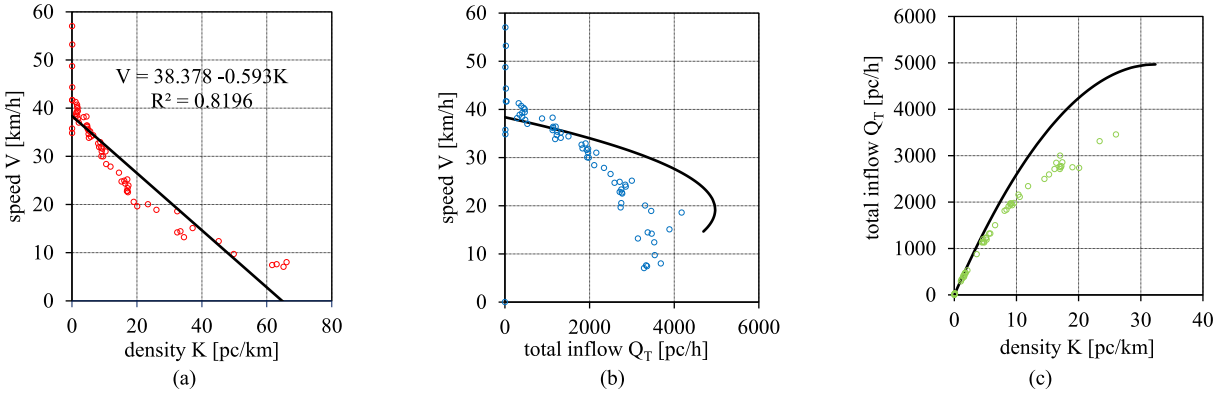

Fig.18. Scatter plots of macroscopic traffic variables and calibrated single-regime Greenshields' traffic model. Flower roundabout (Stop) – *Scenario 1* ("balanced – b").

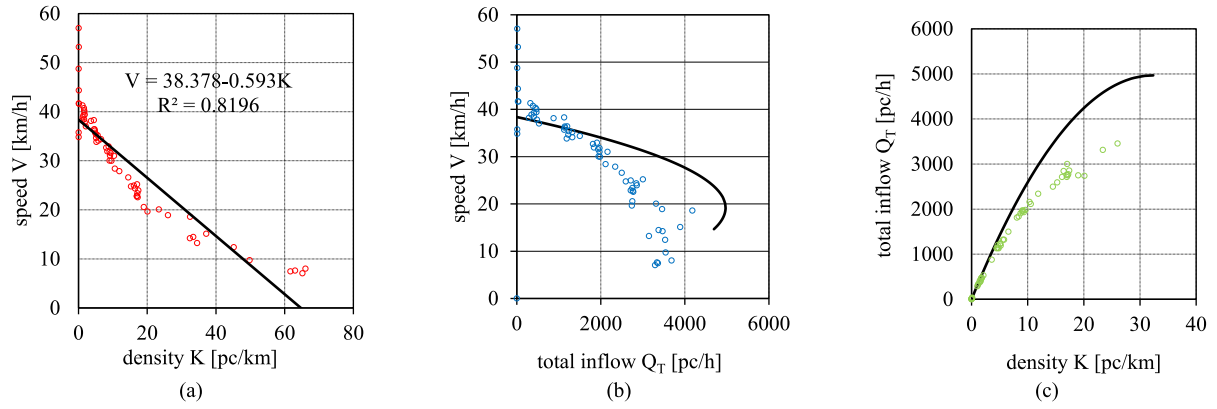

Fig.19. Scatter plots of macroscopic traffic variables and calibrated single-regime Greenshields' traffic model. Flower roundabout (Stop) – *Scenario 2* ("unbalanced – ub").

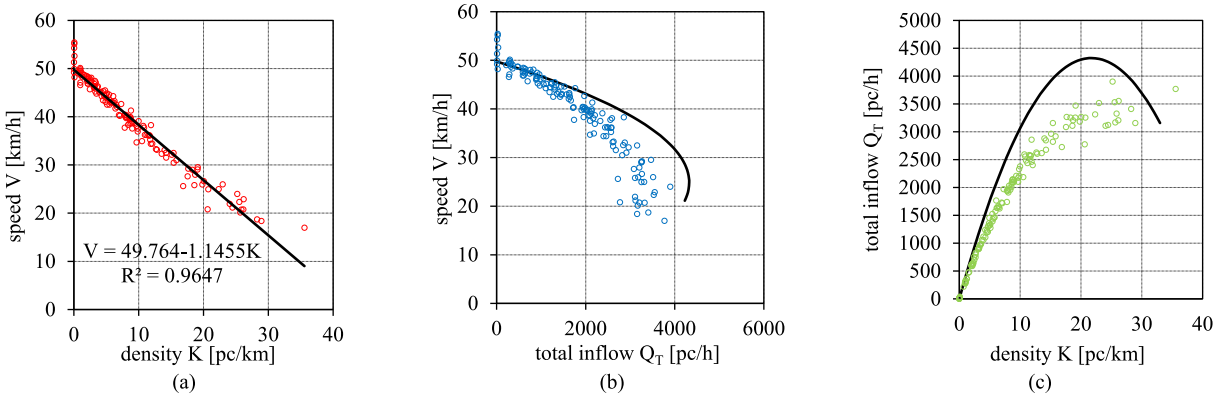

Fig.20. Scatter plots of macroscopic traffic variables and calibrated single-regime Greenshields' traffic model. Turbo roundabout- *Scenario 1* ("balanced – b").

Figs. 22-25 represents the Average delay time (DT) as a function of the total inflow volume Q_T.

DT represents the difference between the predicted travel time (the time interval needed to cross the system under ideal conditions) and the actual travel time. DT is obtained as the mean value of all vehicles within the cordon and transformed into time per kilometre. DT does not incorporate the interval of time wasted in virtual queues.

As is well known, the control delay generally determines LOS at roundabout entries. Average delay time can be regarded as a specific MOE for the whole road intersection, together with the other traffic parameters deducible from the MFD.

Then, outcomes from the present research demonstrate that for conventional layouts, a double-lane roundabout offers the best functionality with reference to DT in comparison to the single-lane roundabout (Figs. 25-28) in all ranges of total inflow. Finally, Figs. 29-33 represents the estimated travel time (TT) curves.

The similarities show that the degree of dispersion between delay and travel times is reasonably high. Regression analysis of the DT data (Figs. 22-26) and TT data (Figs. 27-31) was obtained with the least square method and R^2, which was estimated for the exponential fitting curve.

For the Delay Time (DT), it is possible to deduce the following exponential functional:

$$DT = \psi \cdot e^{\phi \cdot Q_T} \tag{28}$$

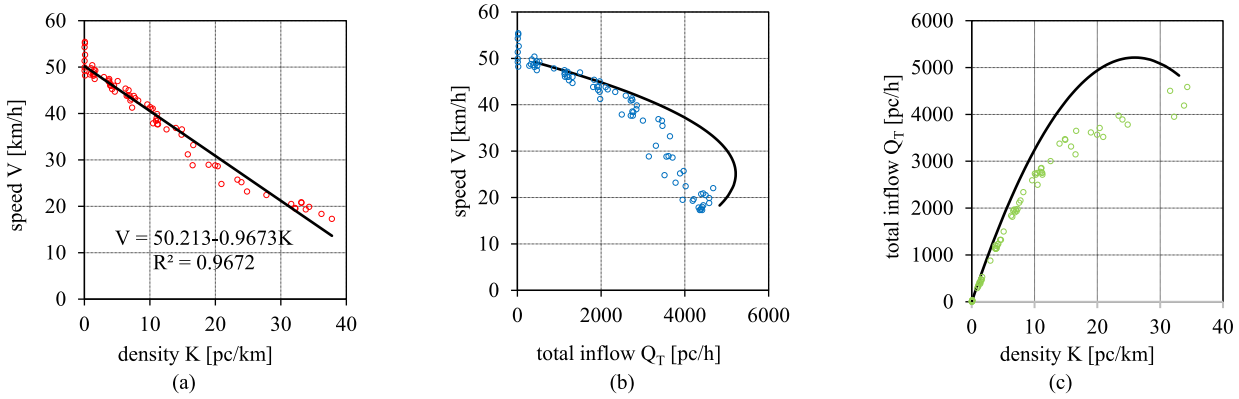

Fig.21. Scatter plots of macroscopic traffic variables and calibrated single-regime Greenshields' traffic model. Turbo roundabout- *Scenario 2* ("balanced – ub").

Table 4
Conventional roundabouts – Values of the macroscopic traffic variables.

Geometric and Traffic Parameters	Single-lane roundabout		Double-lane roundabout	
	Scenario 1	Scenario 2	Scenario 1	Scenario 2
number of entry lanes l	1	1	2	2
number of exit lanes l	1	1	2	2
Number of arms n	4	4	4	4
Speed-density relationship	V=50.436–1.0717 K	V=49.912–0.8113 K	V=49.075–1.4966 K	V=49.692–0.9763 K
R^2	0.9408	0.9278	0.9076	0.9165
Free-flow speed V_f [km/h]	50.44	49.91	49.08	49.69
β [km^2/(pc•h)]	−1.0717	−0.8113	−1.4966	−0.9763
Critical density K_c [pc/km]	23.57	30.76	16.40	25.45
Total capacity C [pc/h]	2374	3071	3233	5058

Table 5
Unconventional roundabouts – Values of the macroscopic traffic variables.

Geometric and Traffic Parameters	Flower roundabout (Yield)		Basic turbo roundabout	
	Scenario 1	Scenario 2	Scenario 1	Scenario 2
number of entry lanes l	2	2	2	2
number of exit lanes l	2	2	1 - 2	1 - 2
Number of arms n	4	4	4	4
Speed-density relationship	V=51.949—0.7458 K	V=43.007—0.861 K	V=49.764–1.1455 K	V=50.213–0.9673 K
R^2	0.9672	0.861	0.9647	0.9672
Free-flow speed V_f [km/h]	51.949	43.007	49.764	50.213
β [km^2/(pc•h)]	−0.7458	−0.861	−1.1455	−0.9673
Critical density K_c [pc/km]	23.87	34.53	21.72	25.96
Total capacity C [pc/h]	4726	7112	4324	5213

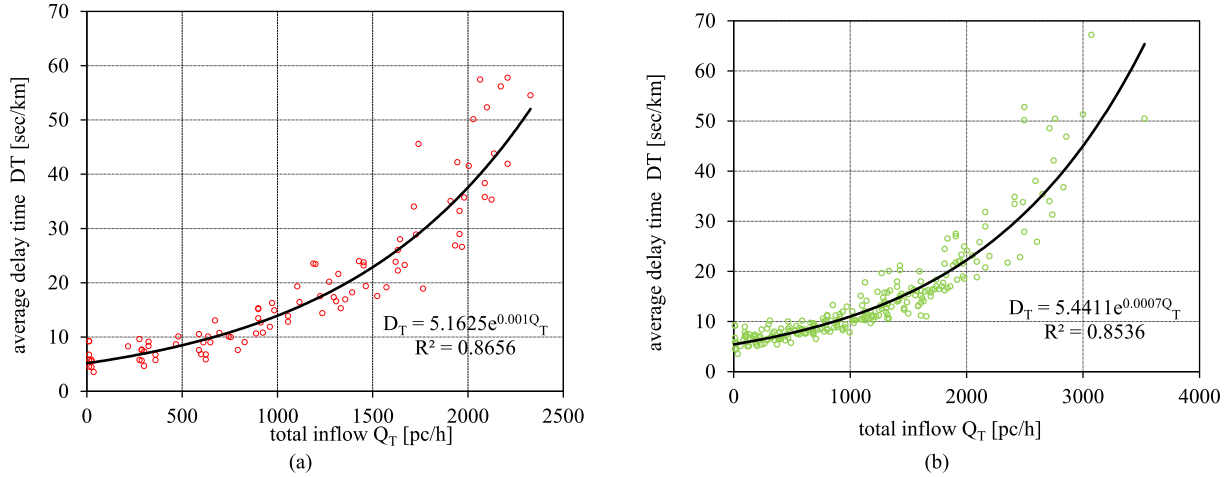

Fig.22. Delay Time as a function of the total inflow volume. Single-lane roundabout. a) Scenario 1; b) Scenario 2.

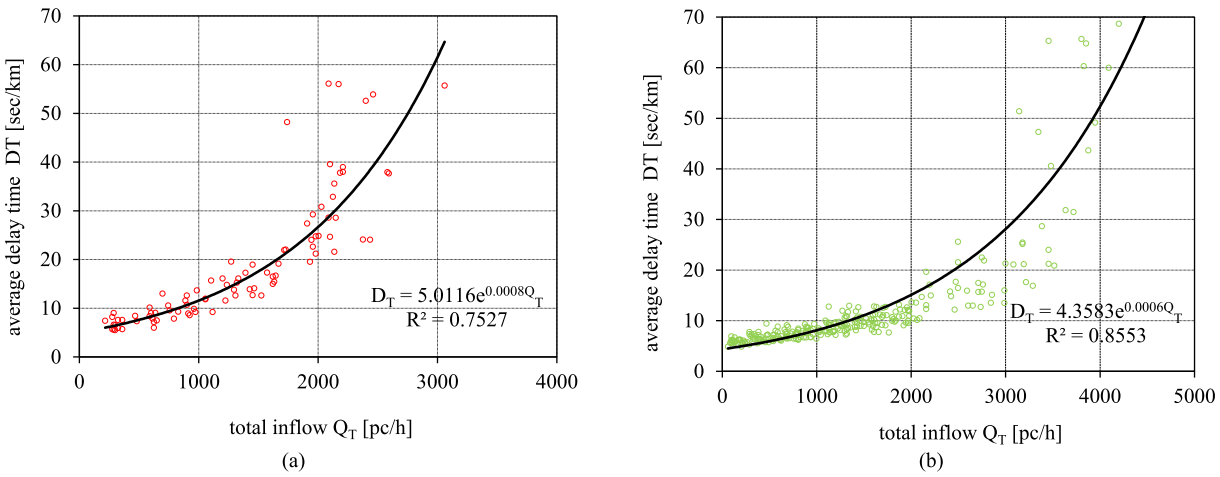

Fig.23. Delay Time as a function of the total inflow volume. Double-lane roundabout. a) Scenario 1; b) Scenario 2.

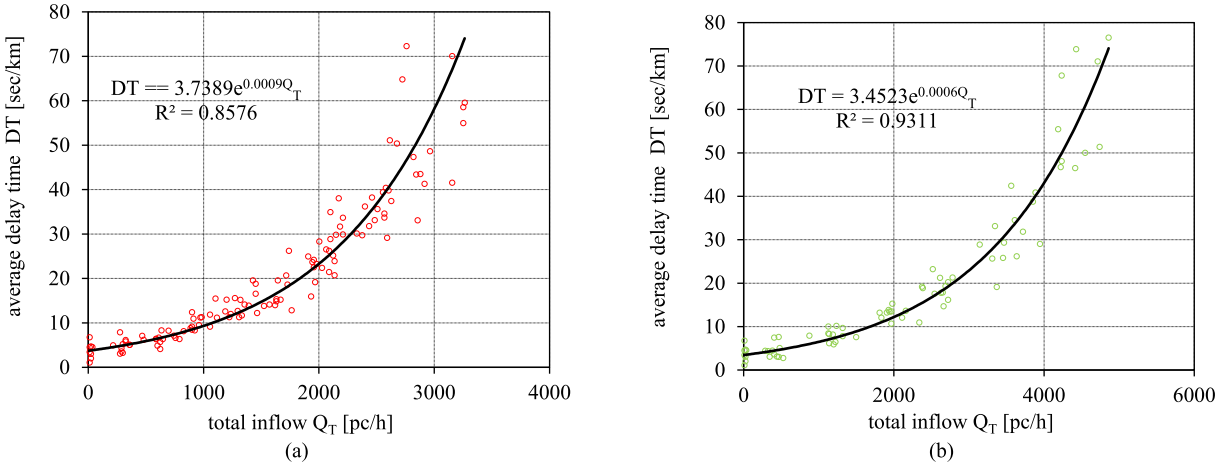

Fig.24. Delay Time as a function of the total inflow volume. Flower roundabout (Yield). a) Scenario 1; b) Scenario 2.

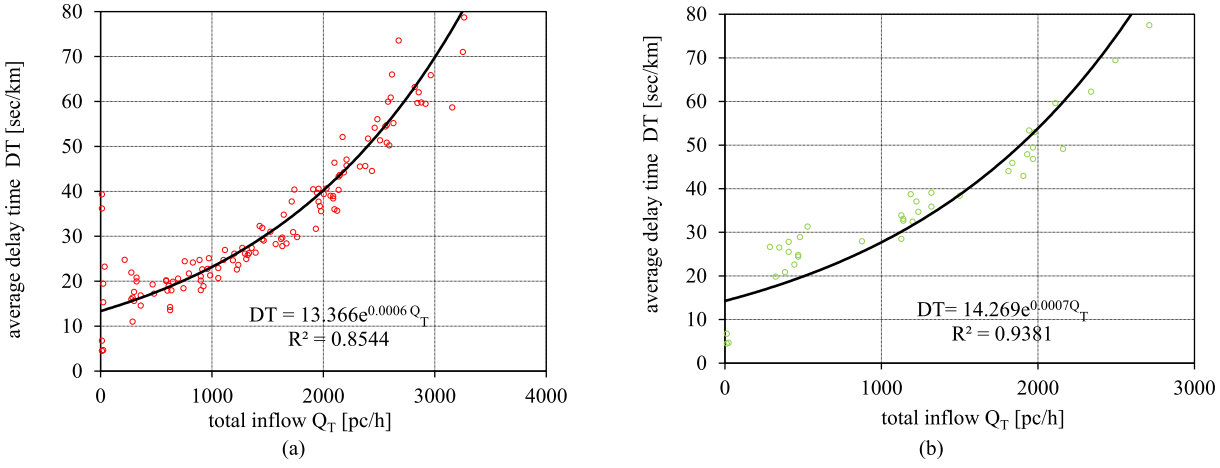

Fig.25. Delay Time as a function of the total inflow volume. Flower roundabout (Stop). a) Scenario 1; b) Scenario 2.

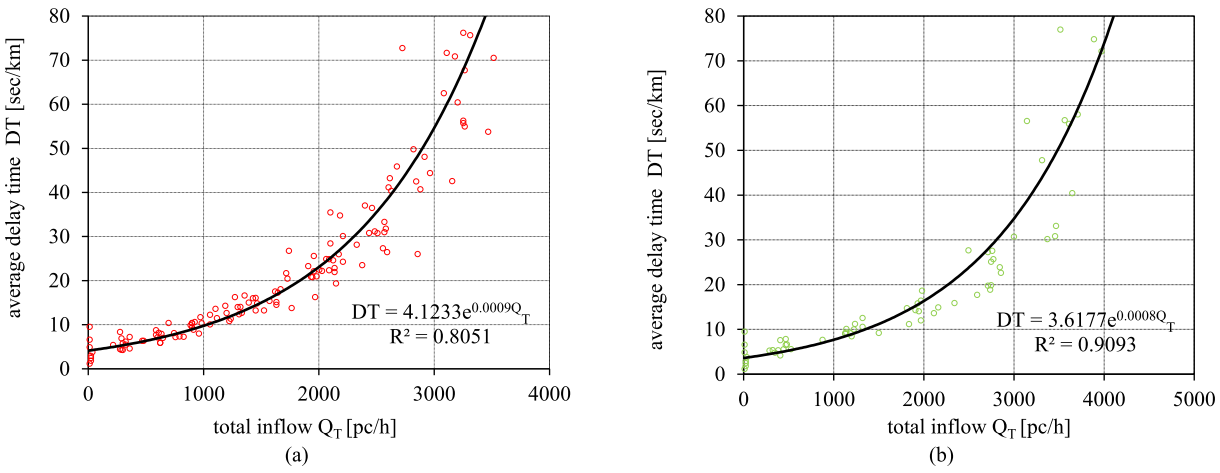

Fig.26. Delay Time as a function of the total inflow volume. Basic turbo roundabout. a) Scenario 1; b) Scenario 2.

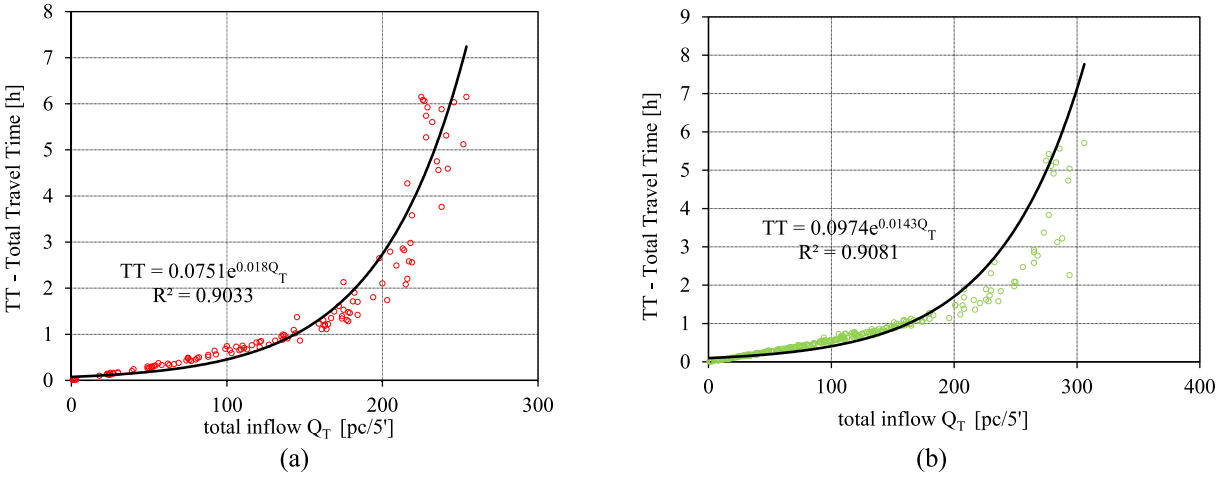

Fig.27. Travel Time as a function of the total inflow volume. Single-lane roundabout. a) Scenario 1; b) Scenario 2.

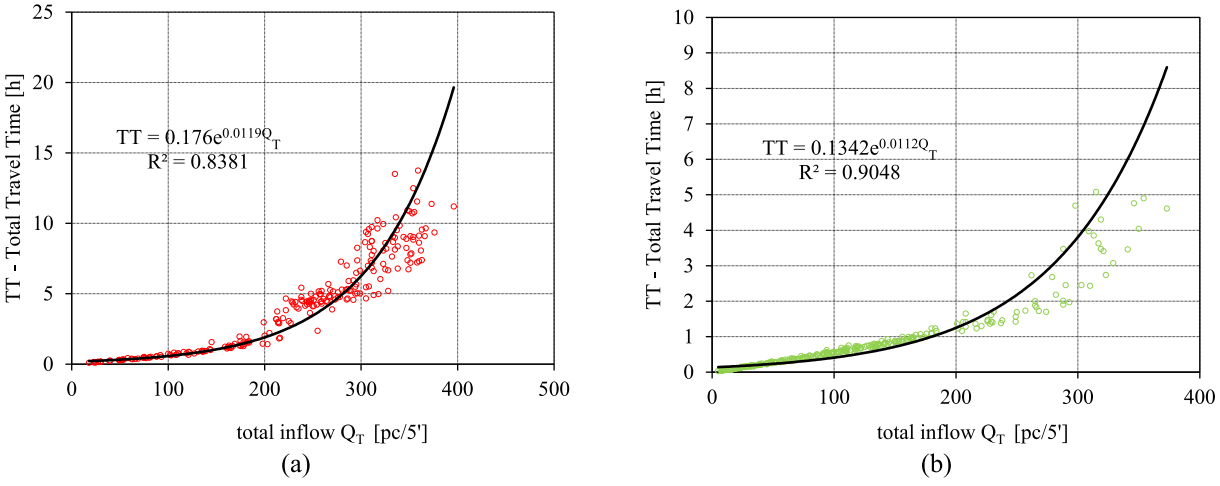

Fig.28. Travel Time as a function of the total inflow volume. Double-lane roundabout. a) Scenario 1; b) Scenario.

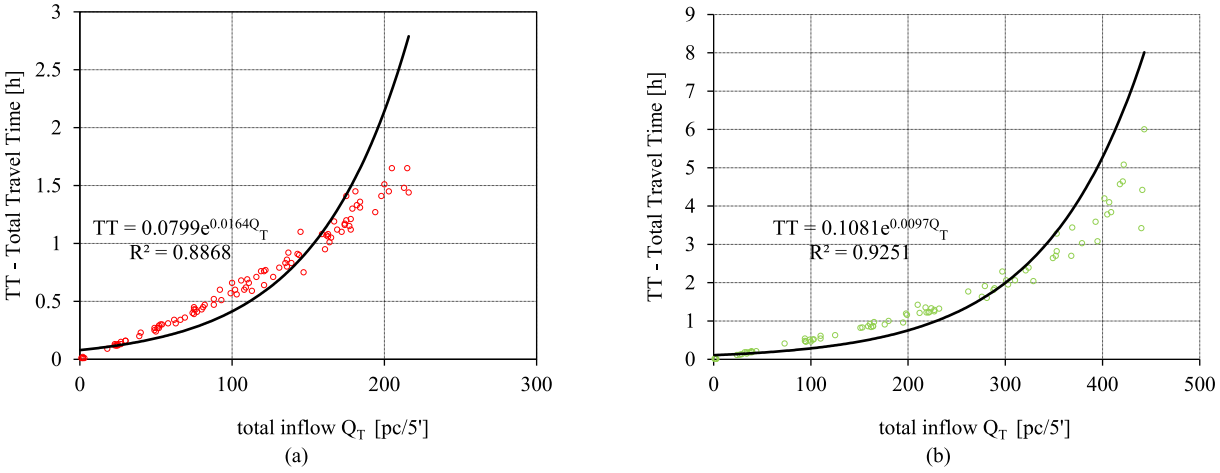

Fig.29. Travel Time as a function of the total inflow volume. Flower roundabout (Yield). a) Scenario 1; b) Scenario 2.

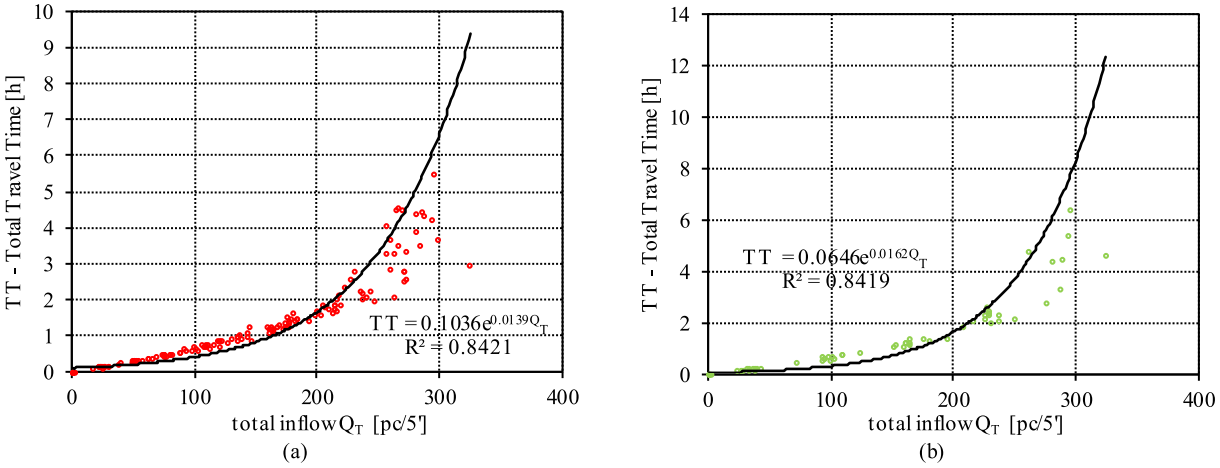

Fig.30. Travel Time as a function of the total inflow volume. Flower roundabout (Stop). a) Scenario 1; b) Scenario 2.

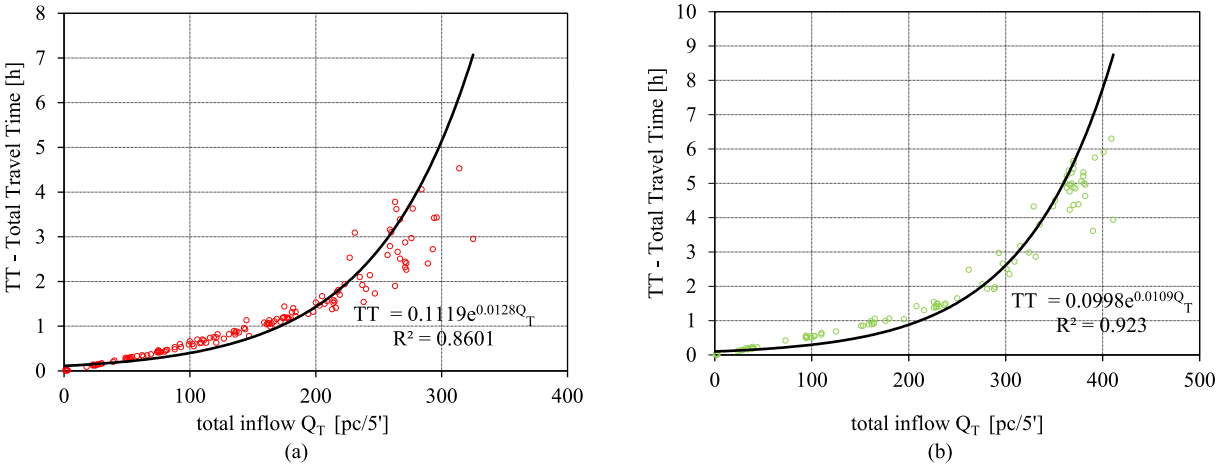

Fig.31. Travel Time as a function of the total inflow volume. Basic turbo roundabout a) Scenario 1; b) Scenario 2.

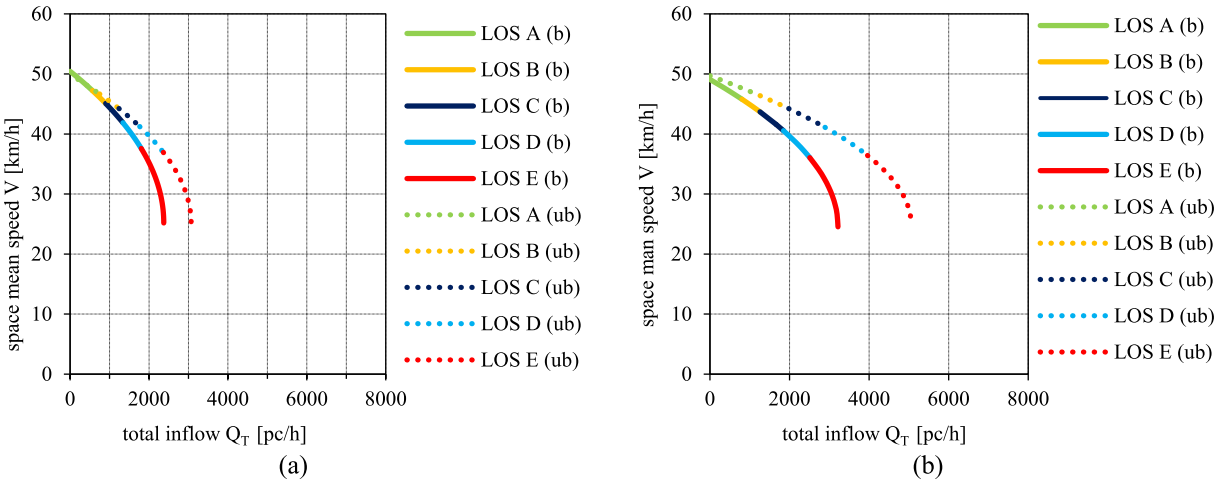

Fig.32. MFDs and LOS limits. a) single-lane roundabout; b) double-lane roundabout.

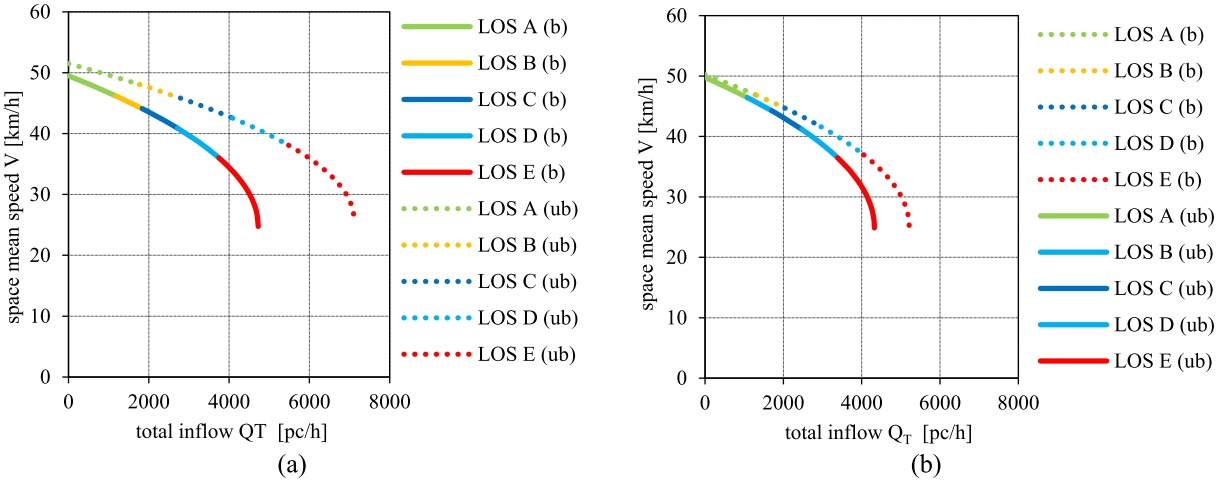

Fig.33. MFDs and LOS limits. a) flower roundabout (Yield); b) Basic turbo roundabout.

Then, the total inflow that gives a given delay time can be estimated by the formula:

$$Q_T = \frac{\ln \frac{DT}{\psi}}{\phi} \tag{29}$$

Similarly, the following relations are deduced for the travel time (TT):

$$TT = \varepsilon \cdot e^{\omega \cdot Q_T} \tag{30}$$

$$Q_T = \frac{\ln \frac{DT}{\varepsilon}}{\omega} \tag{31}$$

The values of the coefficients ϕ, ψ, ε and ω must be read from Figs. 22-31.

Another critical point of view concerns the Levels of Service. As already highlighted, according to the HCM 7th Edition (HCM, 2022), the LOS of the roundabout entries is obtained as a function of the control delay.

Instead, the proposed method is based on the MFDs obtained from a little road network within the analysed cordon. When examining an urban road network with roundabouts, the space mean speed characterizes the LOS. In fact, space mean speed influences the travel time. Therefore, this article uses a criterion for determining LOS based on the MFD. In an MFD of a roundabout (which is a small road network), the following LOS associated with the saturation degrees can be distinguished (HCM 7th Edition):

Table 6
Macroscopic traffic variables as function of LOS – Single-lane roundabout – Scenario 1 ("balanced – b").

LOS	Degree of saturation x		Total inflow Q_T [pc/h]		Mean Speed V [km/h]		Density K [pc/km]	
	min	max	min	max	max	min	min	max
A	0	0.25	0	567	50	47	0	3
B	> 0.25	0.39	567	902	47	45	3	5
C	> 0.39	0.57	902	1340	45	42	5	8
D	> 0.57	0.78	1340	1804	42	38	8	12
E	> 0.78	1.00	1804	2374	38	25	12	24
F	> 1		>2374		< 25		>24	

- $x_A = Q_{TA}$ / C=LOS A density / LOS F density = 0.25;
- $x_B = Q_{TB}$ / C=LOS B density / LOS F density = 0.39;
- $x_C = Q_{TC}$ / C=LOS C density / LOS F density = 0.57;
- $x_D = Q_{TD}$ / C=LOS D density / LOS F density = 0.78;
- $x_E = Q_{TE}$ / C=LOS E density / LOS F density = 1.0.

Consequently, once the saturation degrees are known, it is possible to determine the LOS, whose physical meaning is summarised below:

– LOS A: free flow operation ($x \leq 0.25$);
– LOS B: reasonably unobstructed operation ($0.25 < x \leq 0.39$);
– LOS C: stable flow ($0.39 < x \leq 0.57$);

Table 7
Macroscopic traffic variables as function of LOS – Single-lane roundabout – *Scenario 2* ("unbalanced – ub").

LOS	Degree of saturation x		Total inflow Q_T [pc/h]		Mean Speed V [km/h]		Density K [pc/km]	
	min	max	min	max	max	min	min	max
A	0	0.25	0	747	50	47	0	4
B	> 0.25	0.39	747	1239	47	44	4	7
C	> 0.39	0.57	1239	1765	44	41	7	11
D	> 0.57	0.78	1765	2364	41	37	11	16
E	> 0.78	1.00	2364	3071	37	25	16	31
F	> 1		>	3071	< 25		>31	

Table 8
Macroscopic traffic variables as a function of LOS – Double-lane roundabout – *Scenario 1* ("balanced – b").

LOS	Degree of saturation x		Total inflow Q_T [pc/h]		Mean Speed V [km/h]		Density K [pc/km]	
	min	max	min	max	max	min	min	max
A	0	0.25	0	806	49	46	0	2
B	> 0.25	0.39	806	1258	46	44	2	157
C	> 0.39	0.57	1258	1849	44	41	157	6
D	> 0.57	0.78	1849	2509	41	36	6	9
E	> 0.78	1.00	2509	3218	36	25	9	16
F	> 1		>	3218	< 25		>16	

Table 9
Macroscopic traffic variables as function of LOS – Double-lane roundabout – *Scenario 2* ("unbalanced – ub").

LOS	Degree of saturation x		Total inflow Q_T [pc/h]		Mean Speed V [km/h]		Density K [pc/km]	
	min	max	min	max	max	min	min	max
A	0	0.25	0	1261	50	46	0	3
B	> 0.25	0.39	1261	1981	46	44	3	6
C	> 0.39	0.57	1981	2893	44	41	6	9
D	> 0.57	0.78	2893	3962	41	36	9	14
E	> 0.78	1.00	3962	5058	36	25	14	25
F	> 1		>	5058	< 25		>25	

Table 10
Macroscopic traffic variables as a function of LOS – Flower roundabout (Yield) – *Scenario 1* ("balanced – b").

LOS	Degree of saturation x		Total inflow Q_T [pc/h]		Mean Speed V [km/h]		Density K [pc/km]	
	min	max	min	max	max	min	min	max
A	0	0.25	0	1182	49	46	0	3
B	0.25	0.39	1182	1835	46	44	3	5
C	0.39	0.57	1835	2714	44	41	5	8
D	0.57	0.78	2714	3745	41	36	8	13
E	0.78	1.00	3745	4726	36	25	13	24
F	>	1.00	<	4726	<	25	>	24

Table 11
Macroscopic traffic variables as a function of LOS – Flower roundabout (Yield) – *Scenario 2* ("unbalanced – ub").

LOS	Degree of saturation x		Total inflow Q_T [pc/h]		Mean Speed V [km/h]		Density K [pc/km]	
	min	max	min	max	max	min	min	max
A	0	0.25	0	1769	51	48	0	5
B	0.25	0.39	1769	2787	48	46	5	8
C	0.39	0.57	2787	4085	46	43	8	12
D	0.57	0.78	4085	5483	43	38	12	18
E	0.78	1.00	5483	7111	38	26	18	34
F	>	1.00	<	7111	<	26	>	34

Table 12
Macroscopic traffic variables as function of LOS – Flower roundabout (Stop) – *Scenario 1* ("balanced – b").

LOS	Degree of saturation x		Total inflow Q_T [pc/h]		Mean Speed V [km/h]		Density K [pc/km]	
	min	max	min	max	max	min	min	max
A	0	0.25	0	1090	43	40	0	3
B	0.25	0.39	1090	1657	40	38	3	5
C	0.39	0.57	1657	2449	38	36	5	9
D	0.57	0.78	2449	3341	36	32	9	13
E	0.78	1.00	3341	4296	32	21	13	25
F	>	1.00	<	4296	<	21	>	25

Table 13
Macroscopic traffic variables as function of LOS – Flower roundabout (Stop) – *Scenario 2* ("unbalanced – ub").

LOS	Degree of saturation x		Total inflow Q_T [pc/h]		Mean Speed V [km/h]		Density K [pc/km]	
	min	max	min	max	max	min	min	max
A	0	0.25	0	1259	38	36	0	4
B	0.25	0.39	1259	1917	36	34	4	7
C	0.39	0.57	1917	2844	34	32	7	11
D	0.57	0.78	2844	3877	32	28	11	17
E	0.78	1.00	3877	4968	28	19	17	32
F	>	1.00	<	4968	<	19	>	32

Table 14
Macroscopic traffic variables as function of LOS – Basic turbo roundabout – *Scenario 1* ("balanced – b").

LOS	Degree of saturation x		Total inflow Q_T [pc/h]		Mean Speed V [km/h]		Density K [pc/km]	
	min	max	min	max	max	min	min	max
A	0	0.25	0	1311	50	47	0	4
B	0.25	0.39	1311	2038	47	45	4	6
C	0.39	0.57	2038	2962	45	42	6	9
D	0.57	0.78	2962	4051	42	37	9	14
E	0.78	1.00	4051	5213	37	25	14	26
F	>	1.00	<	5213	<	25	>	26

- LOS D: less stable condition with increases in delay and decreases in travel speed compared to LOS C ($0.57 < x \leq 0.78$);
- LOS E unstable operation and significant delays ($0.78 < x \leq 1.00$);
- LOS F: extremely low speed and congestion phenomena ($x > 1.00$).

Figs. 32-33 display the MFDs and LOS estimated for the various roundabouts types and scenarios. Finally, Tables 6-15 show the limits of each service level (from A to F) and the related values of the total inflow volume, average speed and vehicle density. It can be noted that the results in terms of LOS are coherent with total capacity outcomes and confirm that single-lane roundabouts provide lower total inflow for a given LOS. Conversely, flower roundabouts provide better LOS for a prefixed total inflow and could be adopted in medium–high traffic level demand areas or when right-turn manoeuvres are not negligible.

Similar to other methods for roundabout performance assessment, evaluating MOEs through MFDs requires accurate measurement of traffic variables. From this point of view, traditional and modern methods, such as the loop detector data estimation (LDD estimation method) and the floating car data estimation (FCD estimation method), assure a precise estimate of traffic variables. It is worth explaining that the outcomes of this research could be used for choosing the better roundabout type (Corriere et al., 2013; Fernandes et al., 2020) to guarantee total capacity and LOS appropriate to the traffic demand of a particular urban or rural area or for selecting proper traffic regulation systems of smart roads and intersections under human-driven vehicles (HDVs) and connected and automated vehicles (CAVs) environments

Table 15
Macroscopic traffic variables as a function of LOS – Basic turbo roundabout – *Scenario 2* ("unbalanced – ub").

LOS	Degree of saturation x		Total inflow Q_T [pc /h]		Mean Speed V [km/h]		Density K [pc/km]	
	min	max	min	max	max	min	min	max
A	0	0.25	0	1077	50	46	0	3
B	0.25	0.39	1077	1700	46	44	3	5
C	0.39	0.57	1700	3385	46	41	5	8
D	0.57	0.78	3385	4324	41	36	8	12
E	0.78	1.00	4324	0	36	25	12	22
F	>	1.00	<	0	<	25	>	22

(Martin-Gasulla and Elefteriadou 2019; Guerrieri 2021; Mohebifard and Hajbabaie, 2021; Jiang et al., 2022; Guerrieri, 2024b; Tumminello et al., 2024).

Conclusions

The macroscopic fundamental diagram (MFD) relates the macroscopic traffic variables (flow, vehicle density, and space mean speed). It is a noteworthy framework for planning, designing and monitoring the roundabout traffic state. This research has developed a methodology to determine an MFD through microsimulation experiments. The following are the main contributions of this research: conventional and unconventional roundabouts are examined by microscopic traffic simulations in the Aimsun environment considering 45 O/D traffic matrices and two traffic distribution scenarios: a) *Scenario 1* in which entry flow from each entry was set to 33,33 % for right turns, 33,33 % for left turns and 33,33 % for through movements; b) *Scenario 2* with a traffic distribution in the proportion 60 % for right turns, 20 % for left-turns and 20 % for through movements. Space mean speed V, vehicle density K and total inflow Q_T estimation allow us to obtain MFDs for all roundabouts and traffic scenarios studied.

Major findings

The most important findings of this research are the following:

- for medium–low traffic demand levels, the inflow and outflow have very similar values;
- inflow is more suitable concerning outflow for MOEs estimation;
- MFDs show that the space mean speed (V) and the total inflow (Q_T) never drop to zero, even for high vehicle density values;
- MFDs are a practical method for assessing critical density K_c, total capacity C and Level of Service (LOS) of roundabouts;
- MFDs are influenced by the traffic intensity and distribution (i.e. on the scenarios) and are not just an intrinsic property of the roundabouts;
- roundabouts give rise to very different total capacity values , which vary in the range 2374 pc/h − 7112 pc/h, in relation to layout and scenario;
- single-lane roundabouts offer lower total inflow for a given LOS; instead, flower roundabouts provide better LOS for a prefixed total inflow and could be adopted in medium–high traffic level conditions.

MFDs allow for the estimation of the performance of a roundabout as a whole, which can be deduced from relatively simple traffic flow measurements (e.g., by floating cars).

In conclusion, MFDs represent an alternative technique for estimating the MOEs at roundabouts. This is because the MFDs allow us to analyse the entire roundabout by studying it as a whole node of a road network and not as a series of conflict areas from entering and circulating flows as in traditional methods.

Research perspectives

This research's findings are very promising regarding the technical applicability of MFDs to roundabouts. MFDs can estimate the effect of introducing a given roundabout type into complex road networks, such as those in urban areas. Therefore, the proposed methodology is suited for application in the design of new intersections or for monitoring roundabouts during operation. However, this research still has limitations, such as the inability to compare the simulation results with a large sample of experimental data. Further studies must be directed to explore the effect of roundabout dimension, cordon amplitude, and traffic stream composition (e.g., percentage of light and heavy vehicles) on MFDs' shape adopting single and multi-regime speed-density traffic models.

CRediT authorship contribution statement

Marco Guerrieri: Writing – review & editing, Writing – original draft, Validation, Software, Methodology, Investigation, Formal analysis, Data curation, Conceptualization.

Declaration of competing interest

The authors declare that they have no known competing financial interests or personal relationships that could have appeared to influence the work reported in this paper.

Data availability

No data was used for the research described in the article.

References

Barcelo, J., 2010. Fundamentals of Traffic Simulation. Springer.

Brilon, W., Wu, N., Schmitz, J., 2023. Fundamental diagram for an intersection: application for a roundabout. Transp. Res. Rec. 2677 (7), 359–372.

Buisson, C., Daamen, W., Punzo, V., Wagner, P., Montanino, M., Ciuffo, B., 2014. Calibration and validation principles. Traffic Simulation and Data: Validation Methods and Applications 89–118.

Coropulis, S., Berloco, N., Gentile, R., Intini, P., Ranieri, V., 2024. Traffic microsimulation for road safety assessments of vehicle automation scenarios: model comparison and sensitivity analysis. Simul. Model. Pract. Theory 130. https://doi.org/10.1016/j.simpat.2023.102868.

Corriere, F., Guerrieri, M., Ticali, D., Messineo, A., 2013. Estimation of air pollutant emissions in flower roundabouts and in conventional roundabouts. Arch. Civ. Eng. 59 (2), 229–246.

DMRB. 1996. Design manual for roads and bridges, vol. 12, Traffic appraisal of road schemes, Section 2.5, Part I, Traffic appraisal in urban areas. Highway Agency, The Stationery Office, London.

Fernandes, P., Coelho, M.C., 2023. Can turbo-roundabouts and restricted crossing U-Turn be effective solutions for urban three-leg intersections? Sustain. Cities Soc. 96, 104672.

Fernandes, P., Tomás, R., Acuto, F., Pascale, A., Bahmankhah, B., Guarnaccia, C., Granà, A., 2020. Impacts of roundabouts in suburban areas on congestion-specific vehicle speed profiles, pollutant and noise emissions: an empirical analysis. Sustain. Cities Soc. 62, 1.

Gellelli, V., Iuele, T., Vaina, R., 2016. Conversion of a semi-two lanes roundabout into a turbo-roundabout: a performance comparison. Procedia Comput. Sci. 83, 393–400.

Gellelli, V., Iuele, T., Vaina, R., Vitale,, 2017. Investigating the transferability of calibrated microsimulation parameters for operational performance analysis in roundabouts. J. Adv. Transp. https://doi.org/10.1155/2017/3078063.

Gerlough, D.L., Huber, M.J. 1975. Traffic flow theory; A Monograph, Special Report 165. TRB.

Geroliminis, N., Daganzo, C.F. 2007. Macroscopic modeling of traffic in cities, 86th Annual Meeting of the Transportation Research Board, paper # 07- 0413, Washington DC.

Geroliminis, N., Daganzo, C.F., 2008. Existence of urban-scale macroscopic fundamental diagrams: some experimental findings. Transp. Res. B Methodol. 42 (9), 759–770.

Gipps, P.G., 1981. A behavioural car-following model for computer simulation. Transport. Res. Board 15-B, 105–111.

Gipps, P.G., 1986. MULTSIM: a model for simulating vehicular traffic on multi-lane arterial roads. Math Comput Simul 28, 291–295.

Godfrey, J.W., 1969. The mechanism of a road network. Traffic Engineering & Control 11 (7), 323–327.

Greenshields, B.D., 1935. A study of traffic capacity, highway research board. Proceedings 14, 448–477.

Guerrieri, M., 2021. Smart roads geometric design criteria and capacity estimation based on AV and CAV emerging technologies. A case study in the trans-european transport network. International Journal of Intelligent Transportation Systems Research 19 (2), 429–440.
Guerrieri, M., 2024a. A practical method for assessing sustainable traffic levels of roundabouts in urban areas using the macroscopic fundamental diagram. Sustainable Futures 7, 100157.
Guerrieri, M., 2024b. A theoretical model for evaluating the impact of connected and autonomous vehicles on the operational performance of turbo roundabouts. Int. J. Transp. Sci. Technol. 14.
Guerrieri, M., Mauro, R., 2021. Fundamentals of random and traffic processes. Springer Tracts in Civil Engineering 77–102.
Guerrieri, M., Corriere, F., Lo Casto, B., Rizzo, G., 2015. A model for evaluating the environmental and functional benefits of innovative roundabouts. Transp. Res. Part D: Transp. Environ. 39, 1–16.
HCM 7th Edition. 2022. (Highway Capacity Manual, 7th Edition): A Guide for Multimodal Mobility Analysis, TRB.
Hollander, Y., Liu, R., 2008. The principles of calibrating traffic microsimulation models. Transportation 35, 347–362. https://doi.org/10.1007/s11116-007-9156-2.
Jiang, Q., Schroeder, B., Ma, J., Rodegerdts, L., Cesme, B., Bibeka, A., Morgan, A., 2022. Developing highway capacity manual capacity adjustment factors for connected and automated traffic on roundabouts. J. Transport. Eng. Part A: Syst. 148 (5).
Kim, S.J., Kim, W., Rilett, L.R., 2005. Calibration of microsimulation models using nonparametric statistical techniques. Transp. Res. Rec. 1935, 111–119.
Knoop, V., Hoogendoorn, S., Van Lint, J., 2012. Routing strategies based on macroscopic fundamental diagram. Transportation Research Record: Journal of the Transportation Research Board 2315 (1), 1–10.
Lei, Y.-Z., Gong, Y., Yan, X. T. Unraveling stochastic fundamental diagrams considering empirical knowledge: modeling, limitation and further discussion. arXiv: 2404.09318, https://doi.org/10.48550/arXiv.2404.09318.
Martin-Gasulla, M., Elefteriadou, L., 2019. Single-lane roundabout manager under fully automated vehicle environment. Transport. Res. Rec. 2673 (8), 439–449.
Mauro, R., 2010. Calculation of Roundabouts. Springer.
Mohebifard, R., Hajbabaie, A., 2021. Connected automated vehicle control in single lane roundabouts. Transport Res. Part C: Emerg. Technol. 131, 12.
NCHRP Report 672. 2010. Roundabouts: An Informational Guide - Second Edition, TRB.
Ni, D., Hsieh, H.K., Jiang, T., 2018. Modeling phase diagrams as stochastic processes with application in vehicular traffic flow. App. Math. Model. 53, 106–117.
Saffari, E., Yildirimoglu, M., Hickman, M., 2023. Estimation of macroscopic fundamental diagram solely from probe vehicle trajectories with an unknown penetration rate. IEEE Trans. Intell. Transp. Syst. 24 (12), 14970–14981.
Stamos, I., Salanova Grau, J.M., Mitsakis, E., Mamarikas, S., 2015. Macroscopic fundamental diagrams: simulation findings for Thessaloniki's road network. International Journal for Traffic and Transport Engineering 5 (3), 225–237.
Tumminello, M.L., Macioszek, E., Granà, A., 2024. Insights into simulated smart mobility on roundabouts: achievements. Lessons Learned, and Steps Ahead, Sustainability 16 (10), 4079.
Vaiana, R., Gallelli, V., Iuele, T., 2013. Sensitivity analysis in traffic microscopic simulation model for roundabouts. Baltic Journal of Road and Bridge Engineering 8, 174–183.
Zheng, N., Rérat, G., Geroliminis, N., 2016. Time-dependent area-based pricing for multimodal systems with heterogeneous users in an agent- based environment. Transportation Research Part C: Emerging Technologies 62, 133–148.